CONDUCTIVE POLYMER COMPOSITES

Introduction to Electrically Conductive Adhesives

The semiconductor electronic industry has made considerable advances over the past few decades, whereas the essential requirements for interconnects in electronic systems remained unchanged. Electrical components need to be electrically connected for power, ground, and signal transmissions. In spite of the toxicity of lead, lead-containing solder, especially eutectic tin/lead (Sn/Pb) solder alloy, has been the de facto interconnect material in most areas of electronic packaging. These interconnection technologies include pin through hole, surface mount technology (SMT), ball grid array package, chip-scale package (CSP), and flip chip technology (1–3).

With the new emphasis on green, sustainable technologies, research into science and engineering of interconnect materials has changed dramatically. Research efforts have focused on two lead-free alternatives, lead-free metal solder alloys and polymer-based electrically conductive adhesives (ECAs) (4–6). A number of lead-free solder alloys have found their way in commercial products (4–6). However, these lead-free solders possess technical limits, such as processibility, wetting capability, mechanical properties, fatigue, and thermal behavior. Most significantly, current commercially available lead-free solders chosen by the majority of the U.S. electronic industry, such as tin/silver (Sn/Ag) and tin/silver/copper (Sn/Ag/Cu), have higher melting temperatures ($\sim$220°C) than eutectic tin–lead solder (183°C). The higher melting temperatures result in solder reflow temperatures from 230°C to more than 260°C. These higher processing temperatures severely limit the applicability of lead-free solders to organic/polymer packaged components and low cost organic printed circuit boards/substrates. Moreover, the exposure of electronics to higher temperatures degrades component reliability. In addition, high reflow temperatures increase energy consumption and consequently the costs and damage our environment. Some low melting point lead-free alloys have been developed such as Sn/In (T_m, 120°C) and Sn/Bi (T_m, 138°C) (7). However, their material properties and processibility are still of concern.

ECAs are the ideal interconnect alternative to lead containing solder materials. ECA mainly consists of a polymeric resin (epoxy, silicone, polyurethane, or polyimide) that provides physical and mechanical properties such as adhesion, mechanical strength, impact strength, and metal fillers (silver, gold, nickel, or copper) that conduct electricity. Depending on the filler loading level, ECAs can be categorized into isotropically conductive adhesives (ICAs) and anisotropically

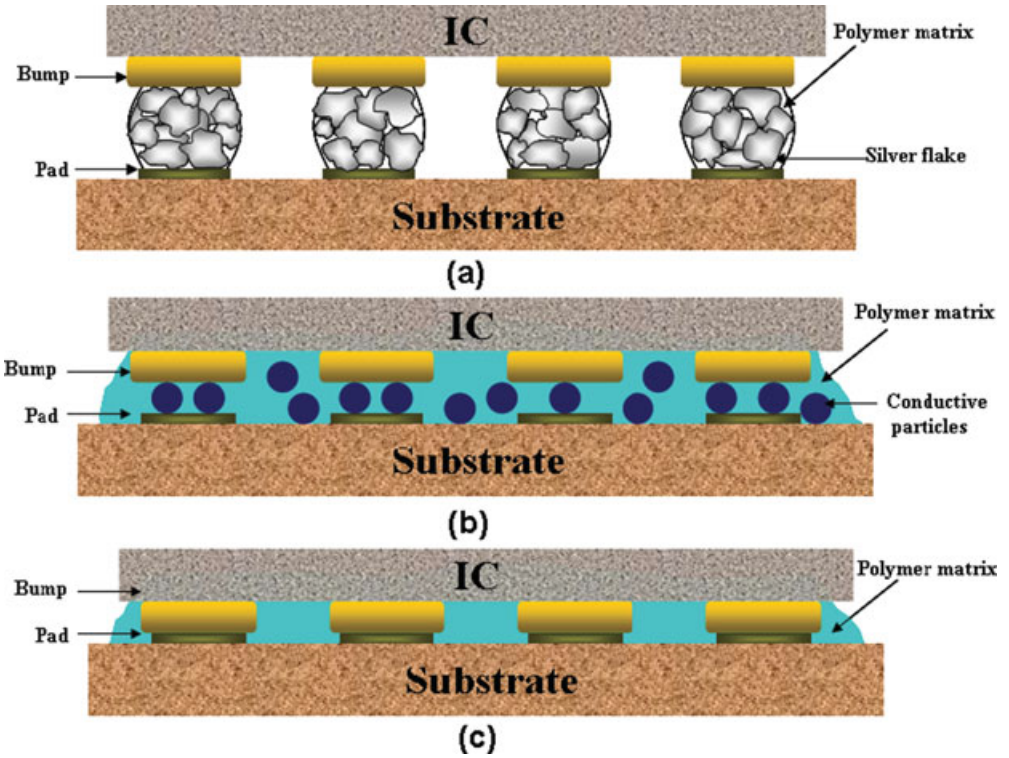

Fig. 1. Schematic illustration of (**a**) ICAs, (**b**) ACAs/ACFs, and (**c**) NCFs.

conductive adhesives/films (ACAs/ACFs) as shown in Figure 1. ICAs are electrically conductive along all the directions. In an ICA, the loading level of conductive fillers (commonly Ag flakes) exceeds the percolation threshold. On the other hand, ACAs/ACFs provide unidirectional electrical conductivity in the vertical or *z*-axis. ACAs/ACFs have a relatively low filler loading. The loading level of ACAs/ACFs is far below the percolation threshold; the low filler loading is insufficient for interparticle contact, which prevents conductivity in the *x*–*y* plane of the adhesives. In addition to ICAs and ACAs/ACFs, nonconductive adhesives/films (NCAs/NCFs) have also been developed recently. Instead of using electrically conductive fillers to establish the conductive joints, the direct and physical contact between two surfaces of the IC bump and the pad of substrates can be made under high bonding pressures and heat. Different adhesives are being adapted as interconnect materials for SMT processes, such as chip on glass, chip on flex, and flip chip bonding technologies in electronic packaging industries.

Compared to metal solder technology, ECAs offer numerous advantages, such as environmental friendliness (elimination of lead usage and flux cleaning), mild processing conditions, fewer processing steps (reducing processing cost), low stress on the substrates, and fine pitch capability due to the availability of small-sized conductive fillers or the development of NCAs/NCFs (2,6,8–10). Polymer-based ECAs can be processed at a much lower temperature (ie, below 150°C) than metal solders. Low processing temperatures of ECAs are compatible with

Table 1. Conductive Adhesives Compared with Solder[a]

Characteristic	Sn/Pb solder	ICA
Volume resistivity, Ω·cm	0.000015	0.00035
Typical junction R, mΩ	10–15	<25
Thermal conductivity, W/m·K	30	3.5
Shear strength, psi	>2200	2000
Finest pitch, mil	12	<6–8
Minimum processing temperature, °C	215	150–170
Environmental impact	Negative	Very minor
Thermal fatigue	Yes	Minimal

[a]Ref. 17.

low cost flexible organic substrates, enabling them to be widely used for the applications in printed electronics, an emerging field with a huge potential market. These applications include organic displays, printed transistors, integrated circuits (ICs), organic light-emitting diodes displays, radio frequency identification tags, sensors, wireless sensor networks, and organic solar cells. For example, ACAs/ACFs have been widely used in LCD display driver chip bonding or for attaching component leads to a matching pad on a thermally sensitive printed circuit board. Because of the low processing temperature of ECAs, energy can be saved for electronic packaging and less hazardous pollutants would be released to the atmosphere. In recent years, intense efforts have been devoted to the fabrication and formulation of flexible electronic materials (substrate, interconnect, etc) to address the dramatically increasing need for high performance, highly compact, and portable devices. The flexible materials offer significant advantages of low profile, lightweight, improved form factor, and high density electronic packaging, attractive for the current and emerging applications in microelectronics (11,12). In particular, flexible interconnects allows for highly integrated systems on flexible substrate materials to be lightweight, thin, bendable, and potentially stretchable enabling the development of more compact end products (11). The preparation of flexible ECAs by selecting flexible and stretchable polymer matrices is promising for these applications (13–16). However, like all other lead-free materials, ECAs have some limitations, such as lower electrical and thermal conductivities compared to solder joints, conductivity fatigue in reliability tests, limited current carrying capability, poor impact performance, and so on (1,2,5,6). Table 1 shows a general comparison between tin–lead solder and generic commercialized ICAs (17). Note that the performance of ICAs is strongly dependent on the filler loading level, polymer matrix, the interaction between fillers and polymer matrix, processing conditions, etc.

In recognition of the importance and challenges of ECAs, worldwide efforts have been devoted to research and development of various high performance ECAs (1–32). The efforts have been focused on material properties and assembly aspects of ECAs. The purpose of this paper is to have a fundamental understanding of the nature of ICAs and their properties and to summarize the significant progress made on the materials research and development for ICA technologies.

Basic Compositions of ICAs

Adhesive Matrix. Polymer matrices are used to form mechanical bonds at an interconnection. Both thermosetting and thermoplastic polymers have been used in ICA formulations. Thermoplastic polymers are rigid materials at temperatures below their glass transition temperature (T_g). Above the T_g, these polymers exhibit flow characteristics. Thus, the T_g of polymer matrices for ICAs must be sufficiently high to avoid polymer flow during the application conditions. Furthermore, the T_g of polymer matrices for ICAs must also be low enough to prevent thermal damage associated with chip carrier and devices during assembly. The main thermoplastic resin used in ICA formulations is polyimide resin. Thermoplastic polymers are particularly advantageous in their ease of processibility and reworkability. A major drawback of thermoplastic ICAs is the degradation of adhesion at high temperatures. Another drawback of polyimide-based ICAs is that they generally contain solvents. During heating, voids are formed when the solvent evaporates. Thermosetting polymers are cross-linked polymers that have an extensive three-dimensional (3-D) molecular structure. The 3-D structure is a result of curing reactions between epoxy resins and hardeners under specific conditions such as heat, UV light, microwave, moisture, and so on. During the curing process, volumetric shrinkage occurs as the distance between molecules changing from van der Waals distance to a covalent distance. The shrinkage during the curing process causes the intimate contact between conductive fillers, contributing to improved electrical conductivity. The ability to maintain strength at high temperatures and robust adhesive bonds are the principal advantages of these materials. However, because the cure reaction is not reversible, rework or repair of interconnections is not an option (33,34). Epoxy resins are the most widely used in thermosetting ICA formulations due to their superior combined properties such as excellent adhesion, chemical and heat resistance, and excellent mechanical properties.

The choice of an adhesive matrix and its formulation is critical to the reliability of ICAs. In practice, many options exist for the adhesive matrix. Besides epoxies, silicones, cyanate esters, and polyurethanes have also been employed in ICA formulations. The general properties of polymer matrices used in ICAs are compared in Table 2 (35). Note that the chemical structure of any polymer matrix can be tailored readily to produce desired properties and to meet requirements for a specific application. An ideal matrix for ICAs should have the following properties: long shelf life (good room temperature latency), fast cure, relatively high T_g, low moisture absorption, and good adhesion.

Electrically Conductive Fillers. Electrically conductive fillers are incorporated into a polymer matrix to render the composite highly electrically conductive. Possible conductive fillers include silver (Ag), gold (Au), nickel (Ni), copper (Cu), and carbon in various shapes and sizes (6). Despite its high cost and electrochemical activity, Ag is the most popular conductive filler for ICAs due to its unique properties. These unique properties include the highest electrical and thermal conductivities of all metals, easy processing into ideal shapes, and significantly higher conductivity of its oxides than those of other metals (6). Although Au does not form oxide at ambient conditions, it is too expensive to be used in

Table 2. Comparison of Adhesives for Electronic Applications[a]

Materials	Advantages	Disadvantages
Epoxies	High-temperature use	Longer cure cycles with anhydride hardeners
	Good moisture and chemical resistance	
	High purity	Degassing required for two-component systems
	Low outgassing	Exotherms in large quantities for amine-curing agents
Silicones	Highest purity	Migrate to other circuit elements
	Stress absorbing	Low surface energy
	High and low temperature stability	Swelled by nonpolar solvents
Polyurethanes	Good flexibility at low temperatures	Lower thermal stability and service temperature than epoxies (150–163°C)
	Stress absorbing	Average bond strength unless primer is used
	Highly versatile chemistry	
Polyimides	Higher temperature stability compared to epoxies	Trapped solvent can produce voids under large ICs Multi-step curing required to volatilize solvent High-stress materials.
	High ionic purity	May absorb moisture in cured condition
	Reduced bleedout	Cannot be B-staged
Cyanate esters	High adhesion strength	High moisture absorption
	High thermal stability High T_g, low CTE	Popcorn susceptibility

[a]Ref. 35.

ICAs. Ni- and Cu-based conductive adhesives generally do not have good conductivity stability because these conductive fillers are easily oxidized. Even with corrosion inhibitors, Cu-based conductive adhesives show a dramatic increase in volume resistivity following aging, especially under elevated temperatures and relative humidities (36). Ag-plated Cu fillers have shown better resistance than Cu fillers, but typically ICAs filled with Ag-coated Cu fillers show increased resistance under aging (37,38). This could be due to the incomplete plating of Cu with Ag, which leads to the oxidation/corrosion of Ag-coated Cu fillers in the polymer matrix and thus the increased electrical resistivity. Only recently, low cost ICAs filled with Ag-coated Cu flakes have been formulated with high reliability (39,40). Ag-filled ICAs typically show stable (or decreased) bulk resistance when exposed to elevated temperatures/relative humidities or thermal cycling tests. Carbon materials such as carbon black (41,42), graphite/graphene (43,44), and carbon nanotubes (CNTs) (45–48) have also been widely used as conductive fillers for conductive polymer composites. To improve the electrical conductivity

of conductive polymer composites, carbon materials have been coated with metals as fillers, such as Ag-plated CNTs (49,50), Ag-plated carbon fibers (51), Ag-coated graphite (52–54), Ni-coated carbon fibers (55), and Ni-coated graphite (56). In addition, to improve electrical and mechanical properties, low melting point fillers have been used in ICA formulations. Conductive filler powders are coated with a low melting point metal. The conductive powder is selected from the group consisting of Au, Cu, Ag, Al, Pd, and Pt. The low melting point metal is selected from the group of fusible metals, such as Bi, In, Sn, Sb, and Zn. The filler particles coated with the low melting point metal can be fused to achieve metallurgical bonding between adjacent particles and between particles and the bond pads that are joined using the adhesive material (57–62).

Metal particles or carbon materials in various shapes and different sizes have been investigated as electrically conductive fillers for ICAs, including micron-sized Ag (or Cu, Ni etc) flakes, nano/micron-sized Ag spherical particles, Ag nanowires, porous nanosized Ag particles, spherical carbon black, micron-sized carbon fibers, carbon nanotubes, nano/micron-sized graphite/graphene. Compared with spherical fillers, higher aspect ratio fillers, especially nanowires/nanotubes, reduce the percolation threshold of conductive polymer composites significantly. Obtaining a low percolation threshold is advantageous in minimizing the filler loading and obtaining ideal mechanical properties of conductive polymer composites. The particle size of ICA fillers generally ranges from 1 to 20 μm. Incorporation of larger particles tends to produce ICAs with a higher electrical conductivity and lower viscosity (63). During the preparation of ICAs, a bimodal mixture of fillers is typically used to increase the packing density and thus the electrical conductivity at a given metal loading. Among these conductive fillers, Ag flakes are the most widely used conductive fillers for ICAs. This is because flakes tend to have a larger contact area and thus a lower contact resistance than spherical fillers.

To obtain good processability, stable dispersions of Ag flakes in a polymer matrix are required. Fatty acids (such as stearic acid) are typically used as a lubricant and compatibilizer to enhance the processability and stability of ICAs. This lubricant layer plays an important role in the dispersion of Ag flakes, viscosity, and the electrical conductivity of ICAs. Therefore, understanding the behavior of lubricants on the surface of Ag flakes is essential for developing high performance ICAs. Lu and co-workers characterized Ag flakes and investigated the thermal decomposition of Ag flake lubricants in detail (64–66). It was found that (*i*) Ag flakes lubricated with fatty acids of different chain lengths have exothermic DSC peaks and mass losses at different temperatures. Ag flakes lubricated with longer chained fatty acids showed exothermic DSC peaks at higher temperatures and started to lose mass at higher temperatures than those lubricated with shorter fatty acids; (*ii*) the lubricant on Ag flake surfaces is a salt formed between the acid and Ag; (*iii*) exothermic DSC peaks (in air) of a lubricated Ag flake are probably due to the oxidation of lubricant layer on the Ag flake surface; (*iv*) the decomposition of the lubricant—Ag salt of fatty acid—includes the release of the fatty acid, formation of short-chain acids by decomposition of hydrocarbon moiety of the fatty acid, and formation of alcohols through decarbonation of the short-chain acids; (*v*) most common solvents such as methanol, tetrahydrofuran, and acetone do not cause significant desorption of the lubricants; (*vi*) addition of

a small amount of two short-chain acids, acetic acid and adipic acid, strongly affects the interaction between the Ag flake and the resin, leading to a significant increase in the viscosity of the ICAs.

The lubricant layer improves the dispersion of Ag flakes within the epoxy resins, which is beneficial for the improvement of electrical conductivity of ICAs. However, the lubricant layer is composed of organic molecules and thus direct metal–metal contact is prohibited. The presence of the lubricant layer increases the tunneling resistance. Removal of lubricants before curing causes the aggregation of Ag flakes. Therefore, it is desired to remove or replace the lubricants with short-chain acids during the curing process. The removal or replacement of the lubricants enables more intimate or direct metal–metal contact between Ag flakes, improving the electrical conductivity of ICAs.

Conduction Mechanisms of ICAs

The formation of electrically conductive paths in ICAs is generally understood by percolation theory. Figure 2 shows the dependence of the resistivity of ICA on the volume fraction of electrically conductive fillers. Increasing filler volume fraction at low filler volume fractions decreases the resistivities of ICAs gradually. As the volume fraction increases a critical volume fraction, that is percolation threshold is reached. At a percolation threshold, conductive fillers come into "contact" and form a continuous linkage between conductive fillers. Consequently, the ICA transforms from an insulator to a conductor. The continuous linkage between conductive fillers should be thought as a series of resistors, as shown in Figure 3. The resistance of an ICA is the sum of filler resistances (R_f) and interparticle contact resistances. The contact resistance is composed of constriction resistance (R_c) and tunneling resistance (R_t). Constriction resistance occurs as the current must squeeze through the small area of contact. Tunnel resistance is due to the intermediate layer between the metal surfaces. Therefore, a total resistance of an ICA, R_{total}, could be written as (67–71)

$$R_{total} = R_f + R_c + R_t \tag{1}$$

where

$$R_f = \frac{\rho}{\pi d} \ln \frac{d + \sqrt{d^2 - D^2}}{d - \sqrt{d^2 - D^2}} \tag{2}$$

$$R_c = \frac{\rho}{d} \tag{3}$$

$$R_t = \frac{\rho_t}{\pi(\frac{d}{2})^2} \tag{4}$$

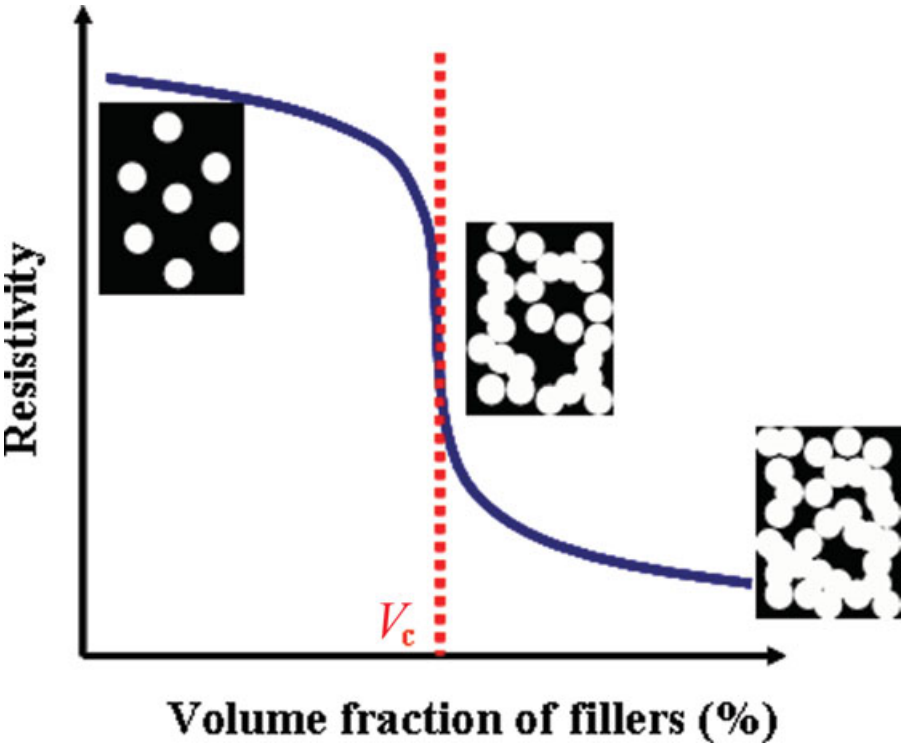

Fig. 2. Dependence of the resistivity of an ICA on the volume fraction of electrically conductive fillers.

$$\rho_t(s,\Phi,\varepsilon) = \frac{10^{-22}}{2}\,\frac{A^2}{1+AB}\,e^{AB} \tag{5}$$

$$A = 7.32 \times 10^{-5}\left(s - \frac{7.2}{\Phi}\right) \tag{6}$$

$$B = 1.265 \times 10^{-6}\sqrt{\Phi - \frac{10}{s\varepsilon}} \tag{7}$$

In equations 2 and 3, ρ is the intrinsic resistivity of conductive fillers, d is the particle diameter, and D is the contact diameter. In equations 4, 5, 6, 7, ρ_t is the tunneling resistivity, s is the thickness of a thin film that separates the conductive fillers, ε is the dielectric of the thin film, and Φ is the work function of the metal fillers.

In an ICA, the particles could be separated by a thin layer of polymer, oxide, or lubricants for most commercial Ag flakes. The thickness of the interface can vary from 10 to 100 Å, depending on the physiochemical properties of the polymer matrix, filler, filler concentration, and the conditions of composite preparation (72,73). Particularly, the filler–polymer interaction energies play a key role in the formation of thin polymer interlayers in interparticle contact regions. For example, if the filler–filler interaction energy is lower than that of polymer matrix, each of the electrically conductive filler will be covered with a thin polymer

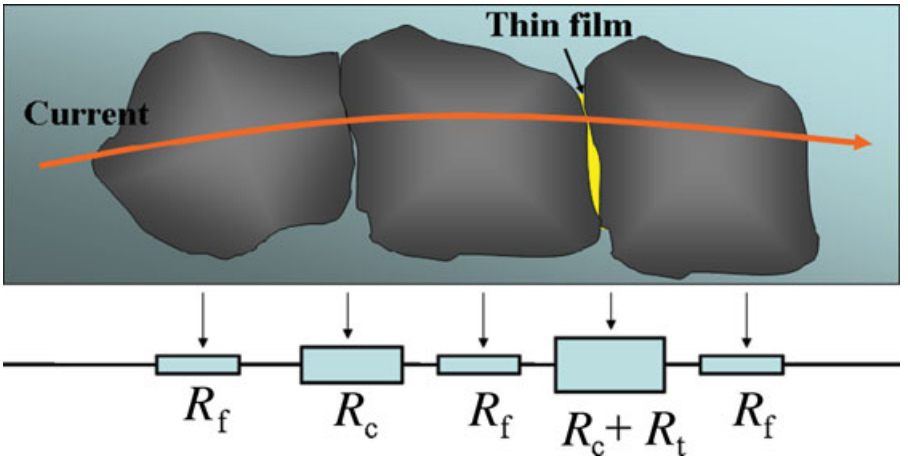

Fig. 3. Electrical resistance of ICAs. The resistance of an ICA is the sum of filler resistances (R_f), constriction resistance (R_c), and tunneling resistance (R_t).

layer. If the filler–filler interaction energy is larger than that of filler–polymer interaction energy, the aggregation of fillers is thermodynamically favored (73).

During the curing process, these interlayers may be squeezed from the interparticle region due to the internal stress caused by cure shrinkage (73); oxide layers may be broken or reduced; the thin layer of lubricants could be removed. In such cases, the direct contact of conductive fillers may occur. There is no clear conclusion regarding whether there is a direct contact between conductive fillers or if there is a thin layer in between them (74). It is possible that both situations coexist within ICAs. The conductivity of an ICA is determined by the composite composition (such as filler loading), the surface properties of conductive fillers (the presence of a thin layer of lubricants or oxide film), physicochemical properties of polymer matrix (cure shrinkage and the interaction between the polymer matrix and conductive fillers), interlayer thickness, temperature, processing conditions of ICAs, etc (73). To achieve conductivity, the volume fraction of conductive fillers in an ICA must be equal to or higher than the critical volume fraction. Similar to solders, ICAs provide the dual functions of electrical connection and mechanical bonding in an interconnection joint. In ICA joints, the polymer resin provides mechanical stability and the conductive filler provides electrical conductivity. Filler loading levels that are too high cause mechanical integrity of adhesive joints to deteriorate. Therefore, the challenge in formulating ICAs is to maximize conductive filler content to achieve high electrical conductivity without adversely affecting the mechanical properties. In a typical ICA formulation, the volume fraction of conductive fillers is about 25–30% (75,76).

Improvement of Electrical Conductivity

Compared with metal solders, polymer-based conductive adhesives have lower electrical conductivity. There is an increasing need for ICAs with higher electrical

conductivity in the electronic industry. Various approaches to formulate highly conductive ICAs have been reported in recent years.

Increase the Polymer Matrix Shrinkage. Adhesive pastes before curing usually have low conductivities. During curing, the epoxy resin shrinks and the conductive fillers within the polymer matrix experience a compressive force. The compressive force brings the conductive fillers closer together and contributes to the improved electrical conductivity of ICAs after curing (77). Formulations with higher cross-linking density have higher cure shrinkage and lower resistivity. For example, by adding 2 and 10 wt% of trifunctional epoxy into the ICA formulation, the resistivity of ICAs decreases from 3.0×10^{-3} to 1.2×10^{-3} and 0.58×10^{-3} Ω·cm, respectively (78).

Incorporation of Short-Chain Diacids and Reducing Agents. As mentioned previously, a lubricant layer is typically present on the surface of commercially available Ag flakes. This thin layer of lubricants plays an important role in the dispersion of Ag flakes in epoxy resins, the viscosity, and the performance of the cured ICAs (64,65). After cure, the configuration of the contacts between conductive fillers is likely metal-lubricant (possibly epoxy)–metal, instead of direct metal–metal contacts. The length and surface orientation of these lubricant molecules affect the electron tunneling/hopping between Ag flakes. *In situ* replacement of long-chain acids (such as stearic acid) with short-chain diacids (such as malonic acid) improves the electron tunneling/hopping between Ag flakes leading to a decrease in resistivity, from $\sim 7.3 \times 10^{-4}$ to $\sim 4.7 \times 10^{-4}$ Ω·cm (79). Li and co-workers also demonstrated that electrical resistivity of ICAs can be decreased from $\sim 7.3 \times 10^{-4}$ to 6.0×10^{-5} Ω·cm by introduction of aldehydes into the formulations (80). The improved electrical conductivity was attributed to the removal of silver oxide and the replacement of long-chain acids (stearic acid) with short-chain acids on the surface of Ag flakes. Both effects reduce the length of the tunneling/hopping gap and may enable direct metallic contacts, improving the electrical conductivity of the ICA.

Incorporation of One-Dimensional Conductive Fillers. High aspect ratio conductive fillers enable the establishment of conductive networks within a polymer matrix at much lower filler loading than that of spherical particles. A low filler loading enables the preparation of highly conductive ICAs without degradation of ICA mechanical properties and processibility. Wu and co-workers reported that the resistivity of ICAs filled with 56 wt% Ag nanowires (30 nm in diameter and a length up to 1.5 μm) was 1.2×10^{-4} Ω·cm, which was significantly lower than that of ICAs filled with 1 μm and 100 nm Ag particles (81). Several possible reasons for the improved electrical conductivity were proposed, including larger contact area, fewer contact points, more stable contact, and enhanced tunneling between these particles due to the presence of a small amount of Ag nanoparticles. Moreover, ICAs filled with Ag nanowires have a better shear strength on an alumina plate (17.6 MPa) than that of ICAs filled with micron-sized Ag particles (17.3 MPa). Similar results were reported by Tao and co-workers (82). Chen and co-workers demonstrated that the resistivity of ICAs could be improved by adding diluents containing Ag nanoparticles and Ag nanowires (83). Besides Ag nanowires, CNTs have also been added to ICA formulations to improve electrical conductivity. Table 3 shows the effect of adding multiwalled CNTs (MWCNTs) on the electrical resistivity of Ag-filled ICAs with different Ag content (84).

Table 3. Electrical Properties of the CNTs/Ag/Epoxy Composites with Different Compositions[a]

Ag (wt%)	45	52	57	66.5	72
Bulk resistivity of ICAs, ρ_1 (Ω·cm)	$\geq 10^8$	6.91×10^6	1.04×10^6	1.01×10^4	1.5×10^{-3}
Bulk resistivity of ICAs with the addition of CNTs, ρ_2 (Ω·cm)	4.8×10^3	3.82×10^1	2.4×10^{-2}	6.47×10^{-3}	1.43×10^{-3}
CNTs (wt%)	1.35	1.0	0.4	0.27	0.24
ρ_1/ρ_2	–	$\approx 10^5$	$\approx 10^8$	$\approx 10^6$	1.05

[a]Ref. 84. (Copyright [2004] IEEE).

The addition of MWCNTs into the formulation improves the electrical conductivity dramatically for ICAs whose filler loading is below percolation threshold. One-dimensional fillers like CNTs improve the contact between conductive fillers and facilitate the formation of 3-D conductive networks. This improved contact between conductive fillers is especially significant prior to reaching the percolation threshold. However, no significant improvement in electrical conductivity is observed when the Ag filler loadings reach the percolation threshold. Oh and co-workers investigated the effect of adding single-walled CNTs (SWCNTs) with different surface properties on the electrical resistivity of a commercial Ag paste filled with 80 wt% Ag powders (49). It was found that the addition of raw SWCNTs into the Ag paste did not improve the electrical conductivity. The addition of an optimized amount (1.5 wt%) of acid-treated SWCNTs can decrease the electrical resistivity significantly. This decrease in resistivity was the result of increased dispersion and p-doping effects. However, the resistivity increased with the addition of more acid-treated SWCNTs. With the addition of Ag-plated SWCNTs, the resistivity of the commercial Ag-filled ICA was decreased by 83%.

Low Temperature Transient Liquid-Phase Sintering. Liquid-phase sintering is a special type of sintering where the liquid phase coexists with the solid particles and the solid phase is soluble in the liquid phase (85). In transient liquid-phase sintering, liquid exists only for a short period of time and then forms an alloy and solidifies. Transient liquid-phase sintering materials enable the assembly process at a low temperature, minimizing stress level while withstanding high temperature joint stability (86). To exploit the advantages of both solder and conductive adhesives, transient liquid-phase fillers have been incorporated into ICA formulations, that is, transient liquid-phase sintered conductive adhesives (59,60,86). The filler used is a mixture of a high melting point metal powder (such as Cu) and a low melting point alloy powder (such as Sn–Pb or Sn–In). The low melting point alloy filler melts during the curing process. The liquid phase forms an alloy with the high melting point particles. The electrical conduction is established through *in situ* formed metallurgical connections between these two types of powders in a polymer binder and between the powders and the metal surfaces (Fig. 4). The polymer binder with acid functional ingredient fluxes both the metal powders and the metal surfaces to be joined. The fluxing process facilitates the transient liquid sintering between the conductive fillers and between the conductive fillers and the metal surface to be joined.

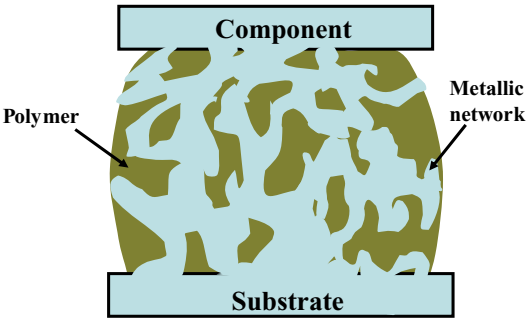

Fig. 4. The joint formed by transient liquid-phase sintered conductive adhesives.

Sintering enables the formation of stable metallic network within the interpenetrating polymer network. Metallurgical bonds between the metallic network within the polymer matrix and the metal surfaces enable good electrical contact, leading to low joint resistance. The polymer binder serves to form mechanical connections and can be tailored to meet the requirements for specific applications. The metallic and polymer networks provide robust electrical and mechanical interconnection. Compared with standard conductive adhesives, transient liquid-phase sintered conductive adhesives exhibit bulk and interfacial resistance comparable to solders and have substantially improved impact strength. Electrical characteristics of transient liquid-phase sintered conductive adhesives remain consistent after reliability tests. Lu and Wong developed an ICA-filled with Ag flakes and low melting point alloy fillers (58). It was found that the ICA showed much lower bulk resistance than the commercial ICA and the control ICA filled with only the Ag flakes. Moreover, the ICA filled with Ag flakes and low melting point alloy fillers showed much lower initial contact resistance (0.15 Ω) than the ICA with only the Ag flakes (∼8.90 Ω) (58). Because of the metallurgical interface between the ICA and the Ni substrate, the contact resistance of the ICA on Ni surfaces remained stable during 85°C/85% relative humidity (RH) aging for 1000 h. Kim and co-workers investigated ICAs composed of fusible Sn–In alloy particles and two type of resins (61). Resin **A** barely wetted Cu surfaces, whereas Resin **B** with reduction capability could flux the metal surfaces and allowed the solder to wet on the Cu. Consequently, Resin **B** with reduction capability was effective at achieving good metallurgical interconnection between the fillers and metallization, producing a low electrical resistance.

The transient liquid-phase sintered conductive adhesives provide the advantages of both conventional soldering technology and conductive adhesives. This hybrid approach produces strong electrical and mechanical interconnections that are resistant to humidity and temperature cycling. One critical limitation of this technology is that the numbers of combinations of low melting and high melting fillers are limited. Only certain combinations of metallic fillers, which are mutually soluble, exist enabling the formation of metallurgical interconnections by transient liquid-phase sintering.

Low Temperature Sintering of Ag Nanoparticles. Low temperature sintering of Ag nanoparticles has been developed as a promising technique for

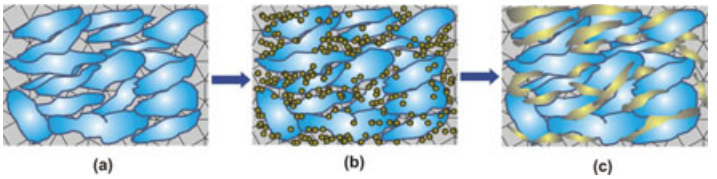

Fig. 5. Schematic representation of ICAs filled with (**a**) Ag flakes, (**b**) Ag flakes and Ag nanoparticles, and (**c**) sintered Ag particles among Ag flakes (105). Reproduced by permission of The Royal Society of Chemistry.

a variety of electronic applications including device interconnect (1,2,87–91), metal–metal bonding process (92), production of conductive tracks (93–96), and electrodes by inkjet printing of Ag inks for semiconductor devices (97). Electrical resistivity of Ag films close to that of bulk Ag (1.6×10^{-6} Ω·cm) has been achieved by sintering of Ag nanoparticles in Ag conductive inks at low temperatures ($<200^{\circ}$C) (98–101). Recently, Ag nanoparticles are proposed to be used as conductive fillers for ICAs in an attempt to improve the electrical conductivity. Figure 5 shows a schematic representation of ICAs filled with Ag flakes, Ag flakes with Ag nanoparticles, and sintered Ag particles among Ag flakes. The addition of Ag nanoparticles increased the number of contact points between conductive fillers. Although the incorporation of Ag nanoparticles decreases the resistivity near the percolation threshold, the addition of Ag nanoparticles into microsized Ag flakes usually increases the resistivity dramatically if no sintering occurs. The increase in resistivity is the result of increased contact resistance (102–105). Through SEM studies, Ye and co-workers observed that addition of Ag nanoparticles into a polymer matrix with micron-sized conductive fillers decreases the chance of direct contact among micron-sized fillers and the contact area between nano- and micron-sized particles is smaller than that between micron-sized particles (103). In addition, the number of contact points significantly increases. As a result, contact resistance of ICAs filled with nano- and micron-sized particles increases as the percentage of Ag nanoparticles increases. However, some research has shown that the electrical conductivity of ICAs can be improved by the addition of Ag nanoparticles (91,104–106).

To develop highly conductive ICAs filled with Ag nanoparticles, it is essential to achieving the sintering between conductive fillers to reduce or eliminate contact resistance effectively within the polymer matrix at low curing temperatures (Fig. 5). Sintering is dependent on many factors such as organic molecules on the nanoparticle surfaces, particle size, pressure, atmospheric gas, temperature, and sintering duration (107). In particular, the removal of organic molecules (or silver oxide) from the surface of Ag nanoparticles plays an important role in sintering onsets, extent of densification, and final grain size (89). The challenges of low temperature sintering ($<200^{\circ}$C) of Ag nanoparticles within the polymer matrix lies in the facts that (*i*) most excellent polymeric dispersants (108–111) (such as polyvinylpyrrolidone) or other small molecules with a long alkyl chain (112,113) cannot be debonded or decomposed at low temperatures. This is a problem because the removal of organic molecules is a prerequisite for sintering to occur; (*ii*) the sintering of Ag nanoparticles in polymer composites is hindered by

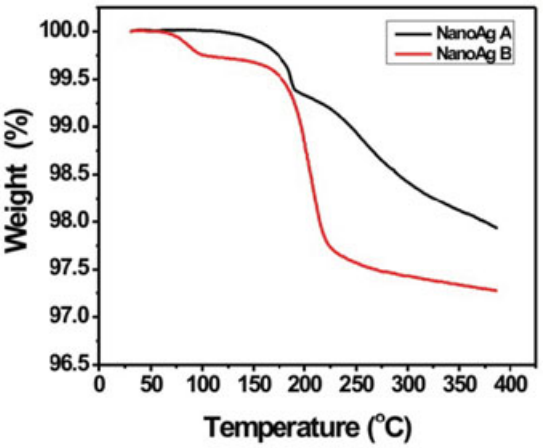

Fig. 6. TGA results of nanoAg **A** and nanoAg **B** (105). Reproduced by permission of The Royal Society of Chemistry.

high volume fraction (typically 70–80 vol%) of highly cross-linked polymer matrices (105). The synthesis of Ag nanoparticles that sinter at low temperatures is critical for the preparation of highly conductive ICAs.

Ag nanoparticles have been widely synthesized by wet-chemical methods. Various stabilizers have been used to prevent the aggregation of Ag nanoparticles and for the control of the size, size distribution, shape, and solubility (110,111). The surfactants used include long-chain carboxylates (112), polyvinylpyrrolidone (102,114), polyacrylamide (110,111), etc. The content of surface residues of Ag nanoparticles synthesized by wet-chemical methods is typically more than 10 wt% (113,115,116). Note that the removal of these stabilizers from Ag nanoparticles before their incorporation into the formulation causes aggregation. The decomposition of surface residues usually occurs at temperatures higher than 250°C (102,110,111,114,115). It is a challenge to produce Ag nanoparticles with a small amount of surface residues that can be decomposed at low temperatures. In recognition of these issues, Ag nanoparticles have been synthesized by combustion chemical vapor condensation (CCVC) method to enable sintering at low temperatures. Figure 6 shows TGA results of two Ag nanoparticles (nanoAg **A** and nanoAg **B**) synthesized by CCVC using the same starting precursor (Ag salt of fatty acid) but under different synthetic conditions. The weight losses for nanoAg **A** and nanoAg **B** at 400°C are 2.06% and 2.73%, respectively. In particular, the decomposition of surface residues of nanoAg **B** is almost finished at 220°C. NanaAg **B** satisfies the two criteria for low temperature sintering, allowing the formation of the metallurgical bonds between the conductive fillers within the polymer matrix and effectively reducing the contact resistance (Fig. 5).

Figure 7 shows the electrical properties of ICAs filled with Ag flakes and nanoAg **A** or nanoAg **B**. When cured at 150°C for 1 h, bulk resistivities of ICAs filled with nanoAg **A** and Ag flakes, and ICAs with nanoAg **B** and Ag flakes are 8.43×10^{-4} and 2.44×10^{-2} Ω·cm, respectively. These resistivities are higher than that of typical ICAs filled with micron-sized Ag flake ($\sim 10^{-4}$ Ω·cm).

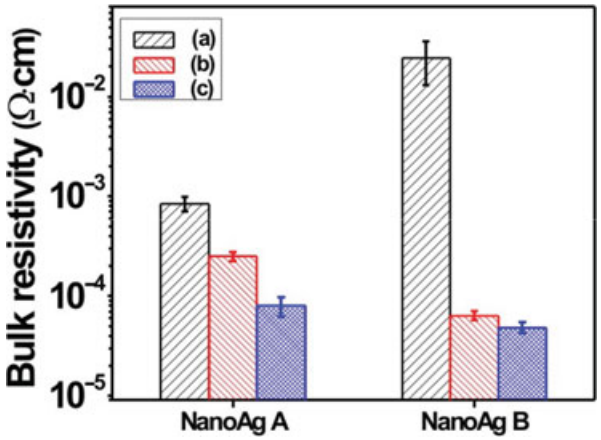

Fig. 7. Bulk resistivity of ICAs filled with nanoAg **A** and Ag flakes and nanoAg **B** with Ag flakes (**a**) cured at 150°C, (**b**) annealed at 180°C after curing, and (**c**) cured at 180°C (105). Reproduced by permission of The Royal Society of Chemistry.

After the samples were annealed at 180°C for 1 h, lower resistivities of both ICAs compared with those cured at 150°C were obtained, resulting from further sintering of Ag nanoparticles. The resistivity of the annealed nanocomposite filled with nanoAg **A** and Ag flakes is several times lower than that of the nanocomposite cured at 150°C. The resistivity of nanocomposite filled with nanoAg **B** and Ag flakes decreases by more than three orders of magnitude following annealing. Figure 8 shows cross-sections of ICAs filled with Ag flakes and nanoAg **B** cured at 150°C for 1 h, annealed at 180°C for 1 h after the curing, and cured at 180°C for 1 h. When nanocomposites were cured at 150°C (Fig. 8**a**), spherical Ag nanoparticles were observed in the polymer matrix. When the samples were annealed at 180°C or cured at 180°C for 1 h (Figs. 8**b** and 8**c**), the morphologies of the nanocomposites changed; spherical Ag nanoparticles became an agglomerated mass, indicating sintering occurred between Ag nanoparticles and between Ag nanoparticles and Ag flakes. More distinct sintering can be seen in Figure 8**d** as some of the nanoparticles grew to form facets. Sintering of the conductive fillers allows the formation of metallurgical bonds between Ag nanoparticles, Ag nanoparticles and Ag flakes, and thus 3-D conductive networks form within the polymer matrix. Consequently, sintering of nanoAg **B** within the polymer matrix at 180°C reduced or eliminated the contact resistance effectively and thus ICAs with very low resistivity could be achieved at 180°C. In addition, ICAs cured at 180°C showed a lower resistivity than ICAs that were annealed at 180°C after curing at 150°C. This is because direct curing of ICAs at 180°C bypasses the low temperature regime and thus is more desirable for the particle growth and the neck formation between the conductive fillers.

Jiang and co-workers investigated the effect of Ag nanoparticles functionalized by different surfactants (S1, S2, S3, S4, and S5) on the electrical properties of ICAs filled with Ag flakes and the Ag nanoparticles (Table 4) (104). It was found that the chain length of the surfactants, the debonding temperature, and the molecular behavior are important parameters to initiate sintering of Ag

Table 4. Effect of Different Surfactant-Treated Ag Nanoparticles on the Resistivity of ICAs[a]

Fillers	Filler loading, wt%	Resistivity, Ω·cm[b]
Untreated Ag nanoparticles	60[c]	5.4×10^{-2}
S1-treated Ag nanoparticles	70	5.4×10^{4}
S2-treated Ag nanoparticles	70	2.4×10^{5}
S3-treated Ag nanoparticles	70	2.4×10^{-4}
S4-treated Ag nanoparticles	70	6.3×10^{-4}
S5-treated Ag nanoparticles	70	4.3×10^{-4}

[a]Ref. 104.
[b]The molar ratio of Ag nanoparticles and surfactants was set as 1:1. The ICAs were cured at 150°C for 90 min.
[c]The untreated particles were unable to be loaded with 70 wt%, due to high viscosity of the mixture.

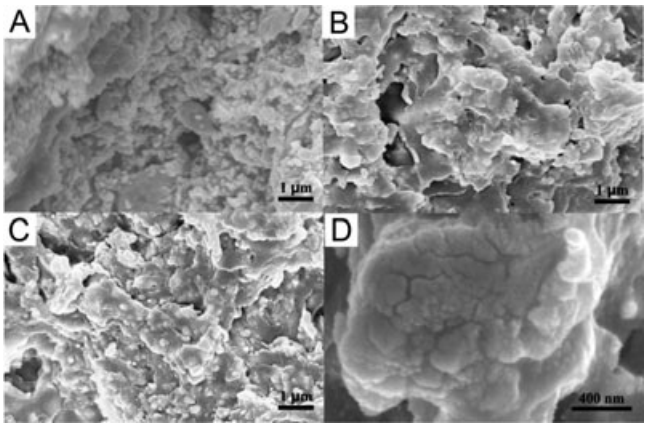

Fig. 8. SEM images of cross-section of ICAs (**a**) cured at 150°C, (**b**) cured at 150°C and then annealed at 180°C, (**c**) cured at 180°C, and (**d**) cured at 180°C at a larger magnification (105). Reproduced by permission of The Royal Society of Chemistry.

nanoparticles in the polymer matrix. These properties of the surfactant dictate the electrical conductivity of the ICA. By using appropriate diacids to functionalize Ag nanoparticles, the resistivity of ICAs filled with Ag flakes and Ag nanoparticles (molar ratio of Ag flakes to nanoparticles is equal to 6:4) was as low as 5×10^{-6} Ω·cm when cured at 150°C for 90 min (91). Morphological studies showed that the decreased resistivity was the result of sintering of Ag nanoparticles within the polymer matrix. Das and co-workers developed Ag-based nano- and micro-filled conductive adhesives for *z*-axis interconnections (87). It was found that with increasing curing temperature, the resistivity of the Ag-filled paste decreased due to sintering of the metal particles. The conductive adhesive cured at 190°C for 2 h showed a resistivity of 2×10^{-5} Ω·cm.

Typically, sintering processes take more than 30 min, limiting commercial viability. Zhang and co-workers have recently demonstrated that ICAs prepared at 230°C for 5 min, at 260°C for 10 min, and using a typical lead-free solder reflow process show electrical resistivities of 8.1×10^{-5}, 6.0×10^{-6}, and

6.3×10^{-5} Ω·cm, respectively (117). The low resistivities obtained are the result of a fast sintering process between incorporated and *in situ* formed nanoparticles on the surface of Ag flakes. The fast sintering is attributed to (*1*) thermal decomposition of silver carboxylates—which are present on the surface of the incorporated silver flakes. The decomposition of silver carboxylate forms silver nanoparticles *in situ*; (*2*) surface activation of the incorporated silver nanoparticles via the removal of surface residues. Both the *in situ* formed and incorporated silver nanoparticles are highly reactive due to their high surface-to-volume ratios and minimal surface residues. These surface properties of the nanoparticles, either incorporated or formed *in situ*, facilitate the fast sintering of silver flakes. Utilizing fast sintering processes, highly conductive ICAs can be prepared within a few minutes. The preparation of highly conductive ICAs during solder reflow reduces the processing steps and cost, enabling the natural integration of ICA technology into standard industrial electronic packaging processes.

Enhancement of Adhesion Strength

One of the major functions of ICAs is to mechanically attach components onto a substrate during assembly. The adhesion strength of bonded interfaces between components and substrates should be able to withstand impact, thermal shocks, thermal cycling, and vibration tests as specified for different applications. One critical reliability issue of ICAs is their lower adhesion strength compared to solder. The adhesion strength of ICAs used to bond different surfaces is dependent on the ability to wet the surfaces and the nature of the bonding mechanism. To achieve maximum adhesion, the adhesive must completely wet the surface maximizing surface coverage and minimizing voids at the interface.

Adhesion Mechanisms. There are two types of adhesion mechanisms, chemical bonding and physical bonding, which contribute to the overall adhesion strength of ICAs on a surface (118). Chemical bonding involves the formation of covalent, hydrogen, ionic, or metallurgical bonds to join components to the substrates (118). Surface modification with coupling agents has emerged as an effective method to enhance adhesion. Coupling agents typically are organofunctional compounds based on silicon (Si), titanium (Ti), or zirconium (Zr). Figure 9 shows some typical coupling agents. A coupling agent consists of two parts and acts as intermediary to "couple" the substrate and polymer. For example, the methoxy or ethoxy groups in silane-coupling agents can be hydrolyzed to form silanol groups. The silanol groups can react with the hydroxyl groups present on the surface of substrates through a condensation mechanism. The other functional groups, such as epoxide and amine groups, can react with epoxy resins or curing agents to form strong covalent bonds during the curing process. Physical bonding involves mechanical interlocking or physical adsorption between the polymer and the surface of substrate. In cases where the molecules of the polymer are highly compatible with the molecules of the substrate, they interact to form an interdiffusion layer. In mechanical interlocking, polymer and substrate interact on a more macroscopic level, where the polymer flows into the crevices and the pores of substrate surface to establish adhesion (118). Therefore, a polymer is expected to have better adhesion on a rougher surface because there is more surface area

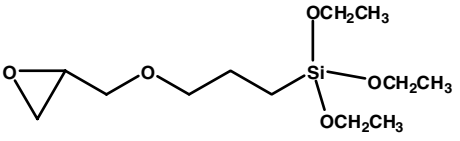

3-Glycidoxypropyl trimethoxysilane (A187)

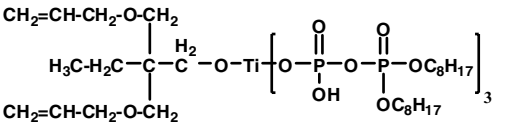

Lica 38

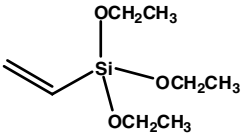

Vinyltrimethoxysilane (A171)

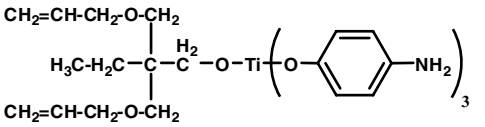

Lica 97

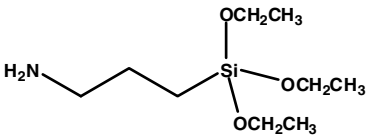

3-Aminopropyl triethoxysilane (A1102)

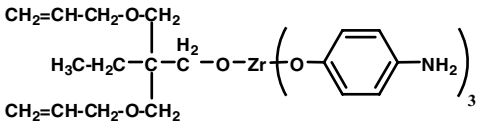

NZ97

Fig. 9. Structures of coupling agents based on silicon, titanium, and zirconium.

and "anchors" to allow for interlocking between the polymer and the substrate. Moreover, the rough adherence surface may enable a better stress transfer from the adherend to the adhesive (119). High adhesion strength is a critical parameter in fine pitch interconnections that are especially fragile to shocks encountered during assembly, handling, and lifetime. Many efforts have been dedicated to improve the adhesion strength to enhance the reliability of fine pitch joints. Since electrical function is needed for ICA interconnects, ICAs are typically used to bond metal surface finishes. In the following section, we focus on the adhesion improvement of ICAs on metal surface finishes.

Adhesion Improvements. Liong and co-workers investigated the adhesion strength of thermoplastic polyarylene ether derivative (PAE-2E)-based ICAs on the surfaces of Sn/Pb, Sn, Cu, and Ni/Au (120). It was observed that the surface roughness and die shear strength were strongly correlated, indicating that adhesion of PAE-2E-based ICAs may be dominated by mechanical interlocking. Adhesions on these surfaces have been improved by incorporation of coupling agents or epoxy blending. With incorporation of a coupling agent, adhesion strength on Ni/Au was approximately 2.75 times the adhesion strength without the coupling agent as a result of chemical interaction at the interface. Figure 10 shows the effect of the combined use of epoxy blending and coupling agents on the adhesion strength of PAE-2 based ICAs on Ni/Au and Sn/Pb surfaces before and after 85°C/85% RH aging (121). The combined use of epoxy blending and coupling agents was effective at increasing the adhesion strength of PAE-2 based ICAs on both Ni/Au and Sn/Pb surfaces before aging. After 85°C/85% RH aging for 168 h, the adhesion strength of PAE-2 based ICAs with the incorporation of

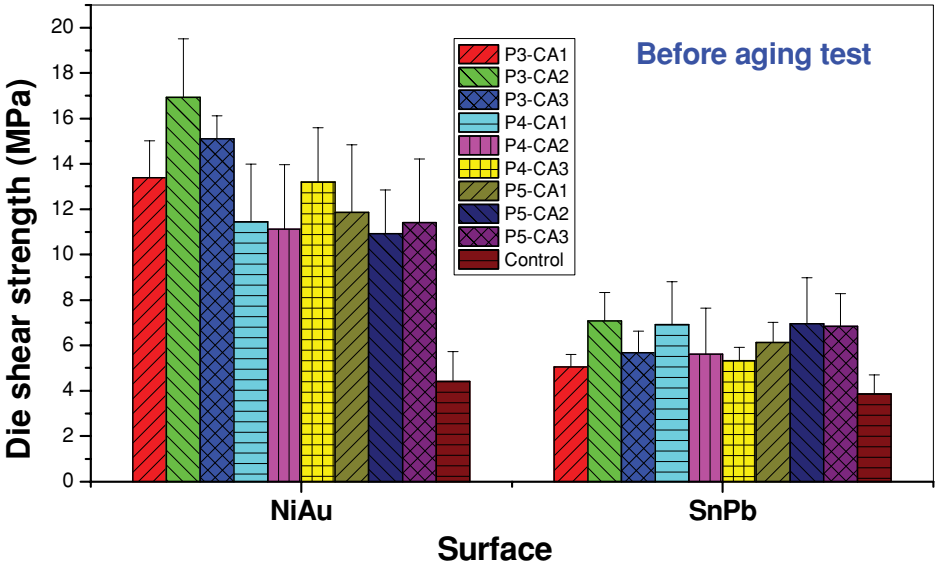

(a)

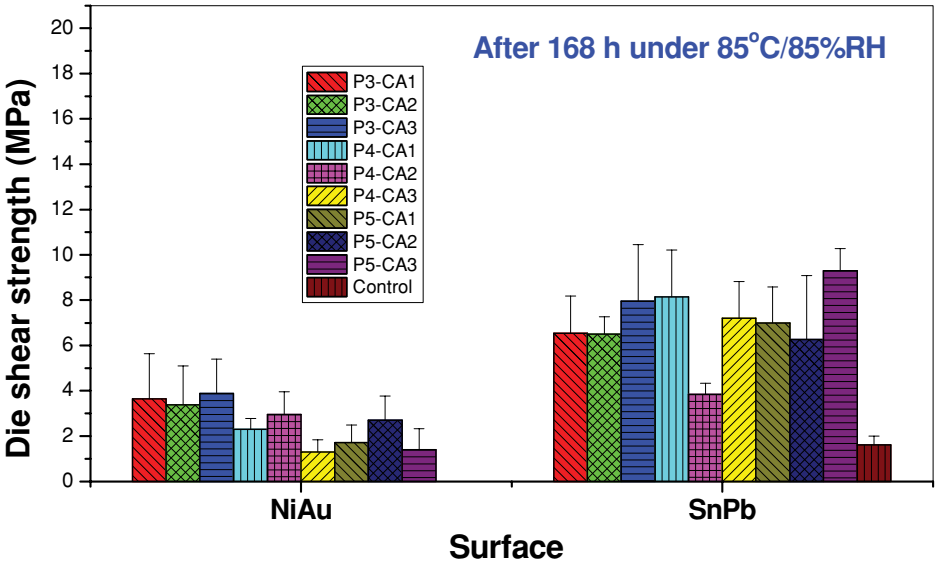

(b)

Fig. 10. Adhesion strength of PAE-2 based ICAs on Ni/Au and Sn/Pb: (**a**) before aging and (**b**) after 85°C/85% RH aging for 168 h. The ratios of epoxy to PAE-2 for P3, P4, and P5 are 1:3, 1:4, and 1:5, respectively. Two amino (CA1 and CA2) and one epoxy (CA3) terminated coupling agents were used as adhesion promoter (121). Reprinted for Ref. 121, copyright 2003, with kind permission from Elservier.

both epoxy and coupling agents on a Sn/Pb surface did not change significantly, whereas the control sample showed a large decrease in adhesion. However, the adhesion strengths on Ni/Au were reduced significantly to less than 50% after 85°C/85% RH aging for 168 h. Factors responsible for these results may involve

Table 5. Functional Groups for Different Surface Finishes[a]

Compound	Formula	Surface finish[b]	Applications
Thiols	R—SH	Au, Ag, Cu, Ni, Sn, Zn, Pt, Ru	Adhesion improvement
Acids	R—COOH	Ag, Fe, Co, Ni, Al	Wetting control
Nitriles	R—C≡N	Au, Ag, Ni, Cu, Pt	Corrosion prevention
Nitrogen-containing compounds	R—NH_2, R_2—NH, R_3N, and others (such as azoles)	Cu, Au	Oxidation retardation
Cyanates	R—N=C=O	Pt, Pd, Rh, Ru	Lubrication
Silanols	R—Si—OH	SiO_2, Al_2O_3, quartz, glass, mica, ZnSe, GeO_2	Wear prevention
Phosphorus compounds	R_3P	Au, CdS, CdSe, CdTe	Chemical sensors and biosensors
	R_3P=O	Co, CdS, CdSe, CdTe	Stabilizer for nanomaterials

[a]Refs. 2 and 123.
[b]R denotes alkyl or aromatic groups.

the hydrophilicity, surface roughness, and interaction between coupling agents (or polymer matrix) and metal surfaces.

A selection of functional groups (ie, coupling agents) plays a key role in the determination of the adhesion strength since different functional groups have a different affinity to a metal surface. Table 5 summarizes the functional groups that may have strong affinities to different metals. To improve the adhesion strength of PAE-2-based ICAs on the surface of Ni/Au at elevated temperatures and relative humidities, thiol compounds, which can form self-assembled monolayers (SAMs) on metal surfaces, have been studied by Moon and co-workers (122). It was found that pretreatment of Ni/Au surface by SAM molecules was more effective at enhancing the adhesion strength than the premixing of SAM molecules with the resin of PAE-2 polymer both before and after aging. Among the SAM molecules studied, SAM molecules containing both thiol and carboxylate groups were the most effective at maintaining the adhesions strength of PAE-2 polymer as well as PAE-2 filled with Ag flakes after aging. Note that the pretreatment of the metal bond by SAM molecules with carboxylate group did not adversely affect the contact resistance stability during aging. Yi and co-workers studied the die shear strength of flexible ICAs, whose matrices were the blend of flexible and rigid epoxy resins, on glass, polyimide, and gold substrates (15). With the increase in the percentage of the flexible epoxy, the adhesion strength continuously decreases on glass and polyimide substrates. Comparing the adhesion strength of flexible ICAs on various substrates, the adhesion strength of flexible ICAs on Au was the lowest when using the same resin formulation. By treating Au substrate with a thiol compound (Fig. 11), Zhang and co-workers showed that the adhesion strength of flexible ICAs on Au and Cu surfaces could

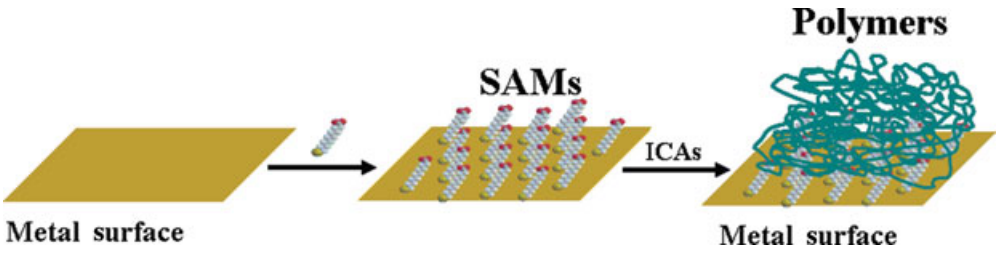

Fig. 11. Self-assembled monolayers (SAMs) used as coupling agents for metal surfaces. One functional group reacts with metal , whereas the other functional group reacts with the polymer during the curing process.

be improved significantly (13,16). The improved adhesion strength resulted from the capability of SAM molecules to strongly bind the metal surfaces and react with the epoxy resin. Compared with other coupling agents, there are two advantages of using thiol compounds for ICA interconnections. First, the formation of SAMs increases the number of molecules on the surface that can react with the polymer during curing, improving adhesion strength. Second, the available conjugated SAM molecules may be beneficial for electron transport at the interface.

Another way to enhance adhesion strength is to use ICAs filled with low melting point fillers, that is, transient liquid-phase sintered conductive adhesives. Transient liquid-phase sintered conductive adhesives have been developed as interconnect materials, enabling the metallurgical bonds to the metal pad and within the conductive fillers (Fig. 4). The joints formed exhibit substantially improved impact strength (59,60).

Reliability Improvements of Contact Resistance of ICAs on Nonnoble Metal Surface Finishes

Despite many advantages of ICAs, one of the critical limitations of ICAs is the unstable contact resistance on nonnoble metal surfaces during the aging at elevated temperatures and relative humidities. Low cost nonnoble metal surfaces such as Sn, Sn/Pb, and Cu are widely used in electronic industry. The National Center of Manufacturing and Science (NCMS) (124) defined the stability criterion for solder replacement conductive adhesives as a contact resistance shift (increase) of less than 20% after aging at 85°C/85% RH for 500 h. However, most commercial ICAs cannot meet the reliability requirement. Two main mechanisms, oxidation and corrosion of the nonnoble metal surfaces, are responsible for the increased contact resistance during reliability tests. Several approaches have been developed to stabilize contact resistance on nonnoble metal surfaces. These approaches include (*i*) the use of purified resins and polymer matrices having low moisture absorption; (*ii*) the incorporation of oxygen scavengers, corrosion inhibitors, low potential metals as sacrificial anode, low melting point fillers, and oxide-penetrating fillers.

Mechanisms Underlying Unstable Contact Resistance. Contact resistance of an ICA joint is composed of the resistance of ICA and the interfacial

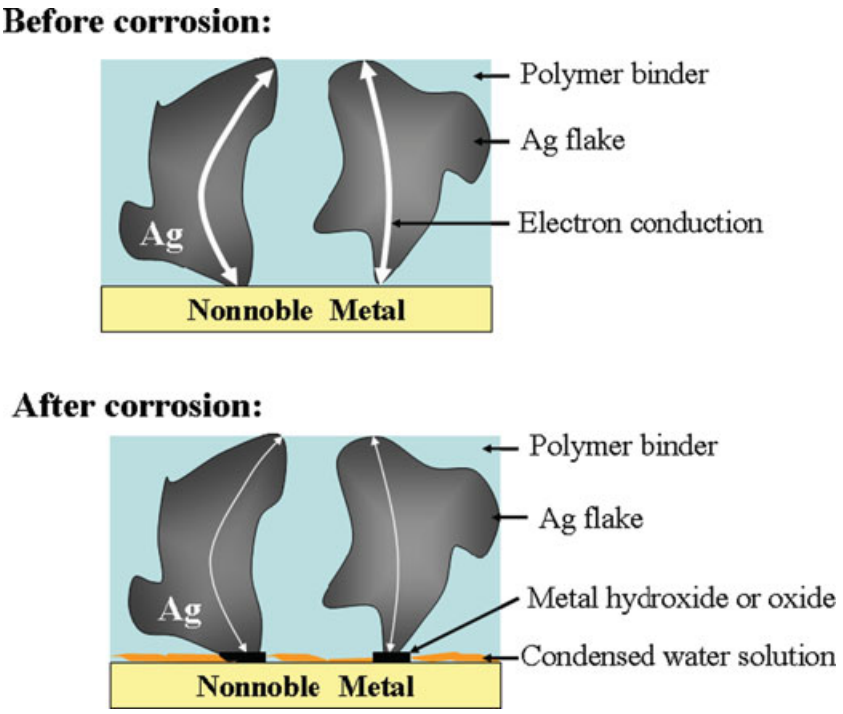

Fig. 12. Metal hydroxide or oxide formation at the interface between an ICA and a nonnoble metal surface due to galvanic corrosion.

resistance between the ICA and metal pads. Most Ag-filled ICAs exhibit stable bulk resistance during aging. Therefore, the unstable contact resistance of ICAs on nonnoble metal surfaces is caused by the increased resistance at the ICA–metal interface. Two main mechanisms, oxidation and corrosion of the nonnoble metal surfaces, have been proposed as the mechanisms underlying unstable contact resistance of ICAs on nonnoble metal surfaces (125). At high temperature/dry conditions, the formation of oxides at ICA–metal interfaces, which are mostly nonconductive, increases the contact resistance of nonnoble metal surfaces during aging. Galvanic corrosion is the second mechanism leading to unstable contact resistance of ICAs on nonnoble metal surfaces (Fig. 12). There are two main requirements for galvanic corrosion to occur: the presence of at least two dissimilar metals (one must be nonnoble) and water with dissolved oxygen and an electrolyte (126). The driving force for galvanic corrosion is a potential difference between different metals. The larger the difference in electrochemical potential, the faster the corrosion develops. Table 6 shows the electrochemical potential values of representative metals. Galvanic corrosion happens only if the potential of a metal, which acts as an anode, is lower than the potential of the cathodic reaction (0.4 V under standard conditions), as shown in equation 8. Therefore, normal potential of Ag, Au, and Pt are higher than the potential of the cathodic reaction. No galvanic corrosion occurs. However, most nonnoble metals such as Ni, Sn, and Sn/Pb have lower potentials than the cathodic reaction. Thus, galvanic corrosion

Table 6. Electrochemical Potential Values for Selected Metals

Element	Reaction	Potential, V
Gold	$Au^+ + e^- = Au$	1.691
	$Au^{3+} + 3e^- = Au$	1.50
Silver	$Ag^+ + e^- = Ag$	0.799
Copper	$Cu^+ + e^- = Cu$	0.521
Oxygen, water	$2H_2O + O_2 + 4e^- = 4OH^-$	0.401
Copper	$Cu^{2+} + 2e^- = Cu$	0.342
Hydrogen	$2H^+ + 2e^- = H_2$	0
Lead	$Pb^{2+} + 2e^- = Pb$	−0.126
Tin	$Sn^{2+} + 2e^- = Sn$	−0.138
Nickel	$Ni^{2+} + 2e^- = Ni$	−0.257
Chromium	$Cr^{3+} + 3e^- = Cr$	−0.744
Zinc	$Zn^{2+} + 2e^- = Zn$	−0.762
Magnesium	$Mg^{2+} + 2e^- = Mg$	−2.372

can occur when the requirements are met. When Ag fillers within an ICA come to contact with a nonnoble metal surface, especially under humid condition (such as 85°C/85% RH aging), moisture and oxygen diffuse into the interface. The moisture present condenses into liquid water, enabling galvanic corrosion to proceed. The accumulated liquid water could dissolve some impurities from epoxy resins or curing agents and form electrolytic solution. All the requirements for galvanic corrosion can be met at the interface. Therefore, galvanic corrosion occurs at the interface. The nonnoble metal (surface finish) acts as an anode and is oxidized by losing electrons to form metal ion (eq. 9). The noble metal (Ag fillers) acts as a cathode, and the reaction occurs as shown in equation 8:

$$2H_2O + O_2 + 4e^- = 4OH^- \tag{8}$$

$$M - ne^- = M^{n+} \tag{9}$$

The reaction between M^{n+} and OH^- forms metal hydroxide, which may further evolve into metal oxide. The formation of metal hydroxide or metal oxide at the interface increases the contact resistance significantly since the metal hydroxide or metal oxide layer is electrically insulating.

To identify the dominant mechanism underlying unstable contact resistance, Lu and co-workers designed a contact resistance test device, which consisted of metal wire segments and conductive adhesive dots (125). Two different samples were tested: Ni flake-filled ICA with Ni wire (referred as Ni/Ni) and Ni flake-filled ICA with Ag wire (referred as Ni/Ag). During 85°C/dry aging, both Ni/Ni and Ni/Ag showed no significant contact resistance increase (Fig. 13). However, during 85°C/85% RH aging, contact resistance of Ni/Ni showed a slight increase but contact resistance of the Ni/Ag combination increased dramatically (Fig. 14). Under 85°C/dry aging condition, no galvanic corrosion happens; therefore, oxidation of the metals is the only possible mechanism. Insignificant contact

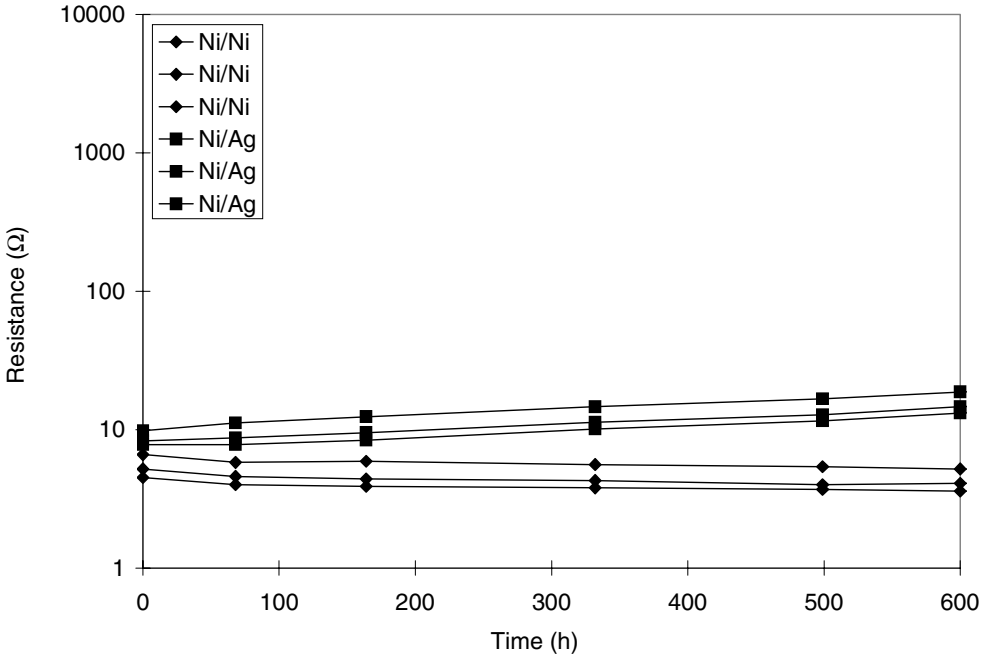

Fig. 13. Contact resistance shifts of a Ni flake-filled ICA with Ni (three samples) and Ag wires (three samples) during 85°C/dry aging (125). Copyright [1999] IEEE.

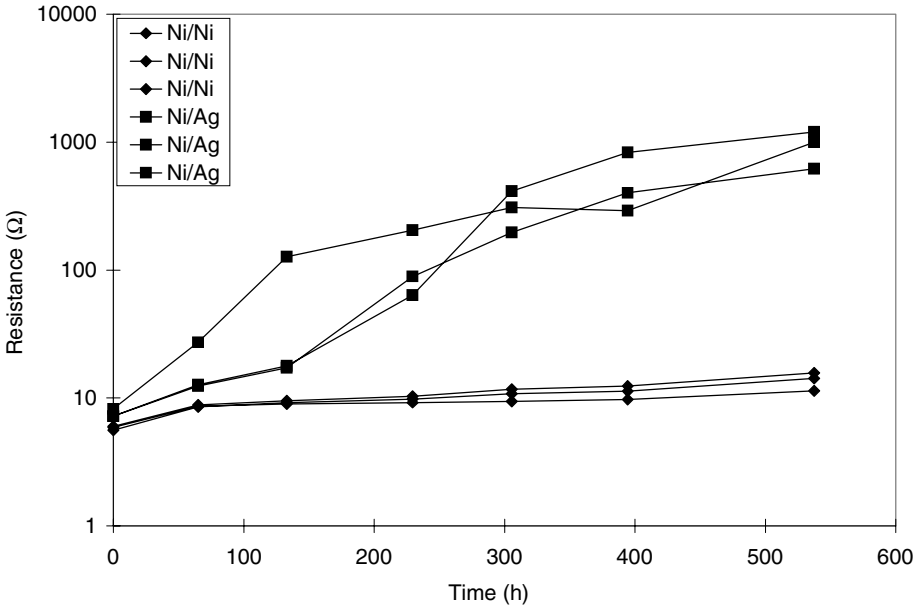

Fig. 14. Contact resistance shifts of a Ni flake-filled ICA with Ni (three samples) and Ag wires (three samples) during 85°C/85% RH aging (125). Copyright [1999] IEEE.

resistance shifts for both samples under 85°C/dry aging condition indicated that oxidation is not dominant at 85°C. Under 85°C/85% RH aging condition, both oxidation and galvanic corrosion can happen. If oxidation dominated, then the Ni/Ni combination should have had larger resistance shift than Ni/Ag combination because Ni is easily oxidized but Ag is not. These results strongly indicate that galvanic corrosion is the dominant mechanism underlying the unstable contact resistance during the aging at elevated temperatures and relative humidities.

Reliability Improvements.

Purified Ingredients and Low Moisture Absorption of Polymer Matrices. Moisture in polymer composites is known to have an adverse effect on both mechanical and electrical properties of epoxy laminates (127,128). The adverse effects of moisture absorption on ICA joints include degradation of mechanical strength, decreasing interfacial adhesion strength, and leading to delamination. The moisture absorption promotes the growth of voids in the joints, giving rise to swelling stress in the joints, inducing the formation of metal oxide layers. Water condenses from the absorbed moisture at the interface between an ICA and metal surface. The condensed water forms an electrolytic solution enabling galvanic corrosion. Therefore, selection of polymer matrices with low moisture absorptions can delay or prevent galvanic corrosion in ICAs. More stable contact resistance on nonnoble metal surfaces was observed with ICAs having low moisture absorption (129).

Impurities such as metal ions in epoxy resins, hardeners, and other ingredients in an ICA formulation may dissolve in the condensed water at the interface between ICA and the nonnoble metal surfaces, forming an electrolyte solution. Dissolved ions increase the electrical conductivity of the solution, accelerating galvanic corrosion. As a result, the contact resistance on nonnoble metal surfaces increases dramatically during the aging at elevated temperatures and relative humidities. ICAs with electrolytes have been shown to increase contact resistance faster on Sn/Pb surfaces (23). Therefore, ICA ingredients such as epoxy resins and hardeners with high purity and the cured polymers with low moisture absorption tend to stabilize the contact resistance of ICAs on the nonnoble metal surfaces.

Oxygen Scavengers. Oxygen scavengers have been added into ICA formulations to slow down the rate of corrosion (130). Ambient oxygen molecules diffuse into the interface between ICA and nonnoble metal surfaces, accelerating galvanic corrosion. Oxygen scavengers incorporated in the formulation react with ambient oxygen molecules and consume them. The reactivity of an oxygen scavenger with oxygen is important. Common oxygen scavengers include hydrazine, carbohydrazide, hydroquinone, gallic acid, propyl gallate, hydroxylamines and related compounds, dihydroxyacetone, 1,2-dihydro-1,2,4,5-tetrazines, erythorbic acid, and oximes (131–134). Note that oxygen can diffuse into the interface when oxygen scavengers are completely consumed. Therefore, the incorporation of oxygen scavengers can only delay, but not prevent galvanic corrosion.

Corrosion Inhibitors. Another way to prevent galvanic corrosion is through the incorporation of corrosion inhibitors into the ICA formulations. Typically, corrosion inhibitors absorbed on the nonnoble metal surfaces form a protective layer of metal complexes. This protective layer acts as a barrier layer between the

metal and its surrounding. To achieve protection of metal surfaces effectively, selection of proper corrosion inhibitors is important. The effectiveness of a specific corrosion inhibitor is highly dependent on the types of metal surfaces. The interaction between metals and corrosion inhibitors plays an important role in the determination of the corrosion inhibition efficiency. Table 5 provides some guidelines for the selection of different functional groups for different metal surfaces. Another important factor is the orientation of corrosion inhibitor molecules on the surface of nonnoble metals. The orientation is important because the bonding strength is highly dependent on the orientation of the molecule on the metallic surfaces. For example, benzotriazole can form stronger bond with Cu surface if oriented parallel to the surface, due to an increased interaction of π-electrons of the ring with vacant d orbitals of Cu (135).

Sacrificial Anode. Using a sacrificial anode is a well-known approach to control galvanic corrosion in the metal industry. Applying more active metals or alloys on a dissimilar metal couple in electrical contact can protect the comparably active metal from galvanic corrosion. When sacrificial anode materials having lower electrochemical potentials than the metals involved in ICA joints (ie, metal fillers in ICA and nonnoble metals), the sacrificial anode materials, instead of the nonnoble metal surface, corrode first, protecting the nonnoble metal surfaces. Theoretically, metals with potentials lower than the active metal in a metal couple can be used as the sacrificial anode materials. However, highly active metals tend to oxidize in air and cannot be used in practice. Among low potential metals, zinc (Zn), aluminum (Al), nickel (Ni), magnesium (Mg), and chromium (Cr) are widely used as sacrificial anode materials. Moon and co-workers investigated the effect of sacrificial anode materials (ie, Zn, Cr, and Mg), the particle sizes and loading levels on the contact resistance stability of ICAs on nonnoble metal surfaces during 85°C/85% RH aging (136). It was found that the addition of Zn and Mg into ICA formulations was very effective at stabilizing the contact resistance of ICAs on Sn, Sn/Pb, and Sn/Ag/Cu surfaces, whereas Cr was not effective due to its strong tendency to self-passivate. To stabilize ICAs on nonnoble metal surfaces, the loading levels of sacrificial anode materials need to be optimized. An excess amount of sacrificial anode materials may generate an excess amount of hydrogen and results in hydrogen blistering or cracking. The optimum amount of sacrificial anode materials is related to the particle size. A lower amount of sacrificial anode materials is needed to suppress galvanic corrosion as the particle size decreases. Li and co-workers investigated the effect of adding Al, Mg, Zn and two Al alloys into the ICA formulations on the contact resistance of ICAs on nonnoble metal surface finishes during 85°C/85% RH aging (126). These nonnoble metal surface finishes include Sn/Pb, Cu, Ni/Au, Sn/Ag, and Sn/Ag/Cu. It was found that the smaller the corrosion potential differences between the ICAs and a surface material, the higher the reliability of the ICA on the metal surface. These results further confirm that galvanic corrosion is the dominant mechanism underlying the unstable contact resistance of the ICAs on nonnoble metal surfaces during 85°C/85% RH aging.

Other Methods. In addition to the above-mentioned methods, other methodologies have been developed to stabilize the contact resistance of ICAs on nonnoble metal surfaces. These methodologies include (*i*) the incorporation of electrically conductive particles with sharp edges for oxide-penetrating, that

is, oxide-penetrating particles: Shrinkage during curing provides the force necessary to drive the metallic particles through the oxide layer penetrating the virgin metal. This concept is used in polymer–solder, which has good contact resistance stability with standard surface-mounted devices on both solder-coated and bare circuit boards (137); (*ii*) incorporation of low melting point fillers: the incorporation of low melting point fillers into ICAs enables the formation of metallurgical bonds between low melting point fillers and nonnoble metal surfaces. ICAs with low melting point fillers have been shown to have stable contact resistances on nonnoble metal surfaces (58).

Low Cost ICAs

One of the main hurdles for the commercial use of current Ag-filled ICAs is the high cost of Ag fillers. Significant research has been devoted to the development of low cost ICAs. Cu could be one of the most promising candidates for low cost electrically conductive fillers, due to its low resistivity, low cost, and reduced electromigration compared to Ag (36,138). Other low cost electrically conductive fillers have also been developed to replace Ag for ICAs, including solder particles (59,139), a mixture of solder and Cu (59), Cu alloys (57,140,141), Cu coated with a thin layer of low melting point metals, Pb-free metals (such as Sn, In, Bi, Sb, Zn, and their alloys) (62), and Ag-coated Cu fillers (37–39,141–143). The challenge associated with ICAs filled with the low cost conductive fillers lies in the oxidation and corrosion of the filler particles during curing and reliability tests. The formation of nonconductive oxides deteriorates the electrical properties of the ICAs, limiting their applications in electronic packaging. Yim and co-workers developed ICAs filled with Cu flakes and investigated the effect of silane-coupling agents (SCAs) on the oxidation prevention of Cu powder (36). It was found that the oxidation of Cu flakes occurred during the curing of Cu-filled ICAs. With the incorporation of the SCA as a corrosion inhibitor, the contact resistance of Cu-filled ICAs dramatically reduced (about 0.3 Ω), compared with Cu-filled ICAs without a corrosion inhibitor (about 100 MΩ). The improvement was attributed to the protection of Cu flakes from oxidation by SCA during the curing at 150°C. However, the developed ICAs showed a significant increase in bulk resistivity, from 1.28×10^{-3} to 3.00×10^{-3} Ω·cm during 85°C/85% RH aging for only 24 h. Cu readily oxidizes even at low temperatures and cannot form a self-protective layer to prevent further oxidation (144,145). Recently, Ho and co-workers investigated the properties of ICAs filled with Cu and Cu alloyed with Ag, Ge, Mg, and Zn in terms of electrical conductivity, thermal stability, and the effects of the trace alloy elements on the oxidation resistance of the metallic fillers (141). The ICAs filled with these fillers showed similar electrical conductivity after curing. However, after exposure at 125°C for 1000 h in air, the resistivity of ICAs filled with Cu alloyed with Ag and Mg increases from 2.38×10^{-4} to 2.43×10^{-3} Ω·cm and from 4.53×10^{-4} to 7.3×10^{-3} Ω·cm, respectively. The resistivity of ICAs filled with other fillers (such as Ge and Zn) increased dramatically.

To enhance oxidation resistance of Cu particles, the effect of coating Cu particles with Ag has been investigated (37–39,141–143). Lin and Chiu reported that a Ag coating on Cu flakes provided good oxidation resistance at temperatures

lower than 175°C (38). However, the resistivity of ICAs filled with the Ag-coated Cu flakes increased from 1.6×10^{-3} Ω·cm before the treatment of the fillers to 2.5×10^{-3} Ω·cm after the heat treatment at 175°C for 2 h as a result of the formation of Cu_2O on the Ag-coated Cu flakes (38). The oxidation of Ag-coated Cu flakes may result from incomplete plating of the Cu flakes with Ag. Park and co-workers investigated the effect of SCAs and dispersing agents on the electrical conductivity and corrosion stability of silicone sealants filled with Ag-coated Cu powders (143). With the most effective SCA, 3-aminopropyltriethoxysilane, silicone sealants filled with the Ag-coated Cu flakes showed a 30% increase in the resistivity after storage at 50°C for 24 h. These results indicate oxidation of the Ag-coated Cu powders at high temperatures. In addition, due to the difference in electrochemical potential between Cu and Ag, galvanic corrosion can occur in pits in the Ag plating. Galvanic corrosion occurs when moisture and oxygen come in contact with the exposed Cu and Ag interface at the edge of the pits. Therefore, the prevention of oxidation and corrosion of the exposed Cu in Ag-coated Cu flakes is crucial for the preparation of highly reliable ICAs filled with Ag-coated Cu flakes.

Various organic corrosion inhibitors have been widely used to retard or prevent the oxidation and corrosion of Cu. The presence of heteroatoms such as nitrogen, sulfur, and phosphorous in organic compounds improves the inhibitor efficiency. This has been explained by the formation of coordinative bonds between vacant d orbitals in Cu atom and atoms able to donate electrons (146). These corrosion inhibitors include azoles (147,148), amines (149–153), amino acids (154), and other compounds (146). The inhibition process generally involves (*i*) the absorption of the corrosion inhibitor on the surface of Cu where Cu undergoes oxidation to Cu^+; (*ii*) the formation of protective insoluble Cu complex on the surface, preventing the Cu surface from oxidation and corrosion. However, the problem is that corrosion inhibitors are thermally unstable at elevated temperatures (155) and excess corrosion inhibitors can degrade the electrical and mechanical properties of ICAs. Recently, many papers have been published on the use of intrinsically conductive polymers (156–159) and their derivatives (157,160,161) as a corrosion inhibitor for Cu. These polymers may function as macromolecular corrosion inhibitors as they reduce the number of active sites on the metal surface through adsorption and may act as a physical barrier by decreasing the transport of corrosive agents (162). But their low processability, poor mechanical properties, and inadequate thermal stability significantly limit their use as corrosion inhibitors (163). Moreover, their insolubility with epoxy resins may further restrict their applications in electronic industry (164).

Very recently, Zhang and co-workers developed highly reliable, highly conductive, low cost ICAs filled with Ag-coated Cu flakes using an amine-based SCA as a corrosion inhibitor (39). It was found that (*i*) incomplete plating of Ag on the surface of Cu flakes exists (Fig. 15); (*ii*) the oxidation of Ag-coated Cu flakes occurs at around 150°C in air and continues up to 600°C. Upon heating to 600°C the Ag-coated Cu flakes weight increased by 22.2%. The onset of oxidation of Ag-coated Cu flakes modified by amine-based SCA is significantly delayed; (*iii*) the ICA filled with Ag-coated Cu flakes modified by the amine-based SCA showed the lowest bulk resistivity of 2.4×10^{-4} Ω·cm, compared with ICAs filled with untreated Ag-coated Cu flakes either with or without the *in situ* incorporation

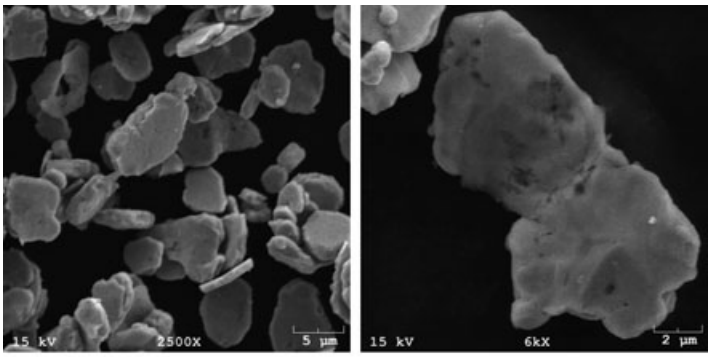

Fig. 15. SEM images of Ag-coated Cu flakes (**a**) and (**b**) (39). Copyright [1999] IEEE.

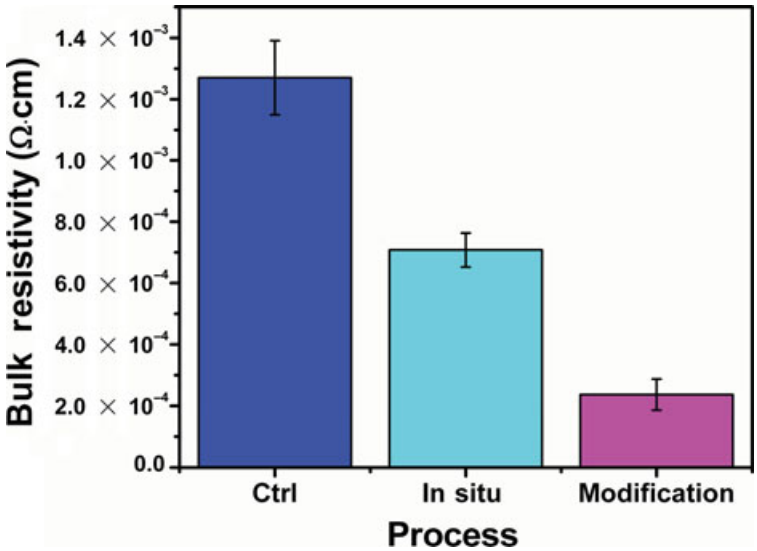

Fig. 16. Electrical resistivity of ICAs filled with (**a**) untreated Ag-coated Cu flakes, (**b**) untreated Ag-coated Cu flakes with *in situ* incorporation of the amine-based SCA, and (**c**) Ag-coated Cu flakes modified by amine-based SCA (39). Copyright [1999] IEEE.

of amine-based SCA, as shown in Figure 16. The main reason for the improved conductivity for ICAs filled with modified Ag-coated Cu flakes is likely the coordination of the nitrogen atom of the amine-based SCA to the exposed Cu of Ag-coated Cu flakes. The coordination protects Cu from oxidation during curing at 150°C. This explanation is supported by the TGA result that Ag-coated Cu began oxidation at the curing temperature (150°C) in the absence of corrosion inhibitor; (*iv*) the contact resistance of Ag-coated Cu flakes increased dramatically after a few hours of 85°C/85% RH aging (Fig. 17). However, the increase in contact resistance of the ICAs filled with modified Ag-coated Cu flakes on a Ni/Au surface was less than 10% after 85°C/85% RH aging for more than 1000 h. The effective

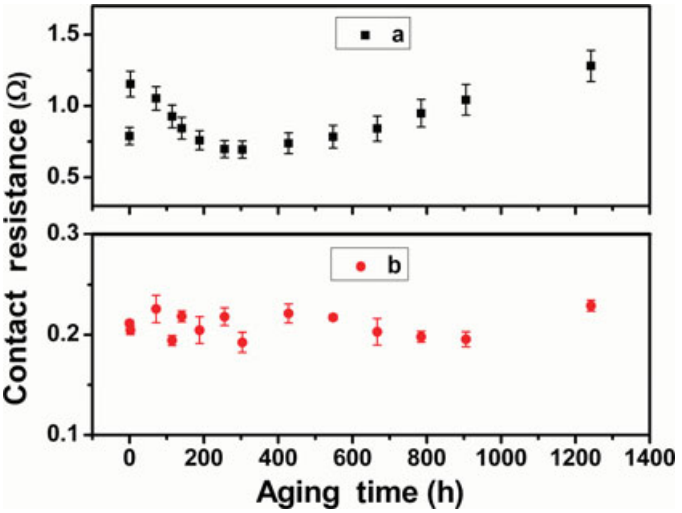

Fig. 17. Contact resistance shifts of ICAs filled with (**a**) untreated Ag-coated Cu flakes and (**b**) Ag-coated Cu flakes modified by amine-based SCA aging at 85°C and 85% RH (39). Copyright [1999] IEEE.

stabilization of contact resistance resulted from the chemical coordination of the amine-based SCA to the exposed Cu of Ag-coated Cu flakes. The amine-based SCA acted as a protective layer, preventing galvanic corrosion. According to the standard set by NCMS (124), the developed low cost ICA is considered highly stable during 85°C/85% RH aging.

Unlike anhydrides, amines that can chemically adsorb and coordinate to Cu (146,165) have been known to be effective corrosion inhibitors for Cu. It has been found that primary amine (150–153), secondary amine (149), and tertiary amine (166) all act as corrosion inhibitors. Using an amine-curing agent for *in situ* oxidation/corrosion protection, Zhang and co-workers reported a novel approach for the preparation of highly reliable, highly conductive, and low cost ICAs filled with Ag-coated Cu flakes (40). The amine-curing agent prevents oxidation of the exposed Cu of Ag-coated Cu flakes during the curing of ICAs at 150°C. After curing, the formed secondary and tertiary amine groups can protect the exposed Cu surface from oxidation/corrosion effectively in harsh environments. The ability of the amine-curing agent to act as corrosion inhibitors prevents oxidation of the Ag-coated Cu flakes, allowing the ICA to maintain stable bulk resistivity during 85°C/85% RH aging.

Most organic corrosion inhibitors may detach or decompose from the metal surfaces at elevated temperatures. The significant advantage of the approaches developed by Zhang and co-workers is the effective protection of the exposed Cu of Ag-coated Cu flakes at very high temperatures. The amine groups used for the protection of Cu from oxidation are chemically linked to the highly cross-linked polymers. This prevents the degradation of the protecting groups at high temperatures. Figure 18 shows the contact resistance shifts of ICAs filled with untreated and treated Ag-coated Cu flakes on a Ni/Au surface after reflows with a peak reflow temperature of 255°C. As Ag-coated Cu flakes started to be oxidized at 150°C,

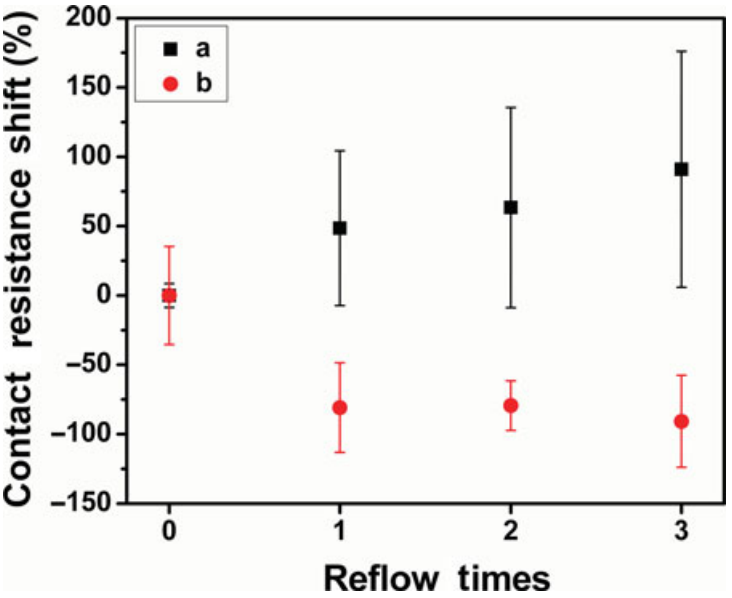

Fig. 18. Contact resistance shifts of ICAs filled with (**a**) untreated Ag-coated Cu flakes and (**b**) Ag-coated Cu flakes modified by amine-based SCA during reflow (39). Copyright [1999] IEEE.

the oxidation of the exposed Cu of Ag-coated Cu flakes led to the increase in contact resistance of ICAs filled with untreated Ag-coated Cu flakes by more than 90% after three reflows. However, ICAs filled with Ag-coated Cu flakes modified by an amine-based SCA showed a decrease in contact resistance. The reaction of the SCA with the epoxy matrix to form highly stable cross-linked polymer networks will prevent desorption/decomposition of the SCA at high temperatures and thus prevent oxidation of the exposed Cu of Ag-coated Cu flakes effectively during reflow. The decreased contact resistance may result from the postcuring effect of ICAs (167,168). The results demonstrated that the developed approach was effective to maintain stable contact resistance at high temperatures.

The key points for the design of highly reliable, highly conductive ICAs filled with low cost conductive fillers involves (*i*) the protection of conductive fillers from the oxidation during curing and reliability tests; (*ii*) the cross-linking of the corrosion inhibitor with epoxy resins enabling the protection of conductive fillers at high temperatures. The development of highly reliable, highly conductive, low cost ICAs will enable their use in electronic packaging.

Applications

Electrically conductive composites have many applications including sensors and actuators (169), nerve regeneration materials (170), transparent conductors (171), electromagnetic shielding (172), and printable conductors (173). However, the main commercial application of conductive composites is for the electronic

packaging industry. The following section discusses in detail the applications of ICAs for die attach and flip chip.

Die Attach Applications. Die attach materials are used to mechanically bond integrated chips to substrates with a high degree of mechanical reliability. In order for integrated chips to function correctly, the die attach material must have electrical, mechanical, and thermal properties compatible with all integrated electronic components. From a mechanical standpoint, die attach materials must have sufficient adhesion to keep the die fixed during device assembly and operation. Thermally, die attach materials must have a thermal coefficient of expansion compatible with other materials to minimize stress. Furthermore, die attach materials must have a sufficient thermal conductivity to dissipate heat during operation. The technical requirements for die attach materials include quick curing, low stress, package crack resistance, and high purity (174).

Prior to conductive adhesives, hermetic die attachment materials consisted of inorganic adhesives: Ag-filled glass, Au/Sn, or Au/Si eutectic. Die attachment with these inorganic materials has a low throughput that cannot be easily adapted to automation. As die size is increasing, processing with inorganic materials is becoming exceedingly difficult. Furthermore, the high temperature glass and eutectic die attach processes create mechanical, thermal, and diffusional stresses that effect device performance. These concerns merit the use of low temperature die attach materials. Polymer-based die attach materials offer many advantages to inorganic die attach materials including lower IC stress due to low modulus (storage and loss), low curing temperatures, manufacturability, and low cost (175). In many cases, die attach also requires electrical contact, in these cases ECAs are used. However, there are many technical issues associated with using ECAs as die attach materials. These problems include package cracking/delamination during reflow, wettability/spreadability with attachment of large dies, void formation, processability with dispensing systems, and polymeric purity. During high temperature ($\sim$245°C), die attachment absorbed moisture within the package expands and vaporizes leading to delamination, fracture, and package cracking. This phenomenon is referred to as the popcorn phenomenon (176). Solutions to popcorn phenomenon have been achieved by introduction of hydrophobic sections within the polymer chain. Recently, industry has moved away from epoxy-based adhesives to cyanate ester based die attach adhesives (2). The use of cyanate-based thermosets as adhesives for die attach is advantageous because cyanate-based adhesives have high thermal stability, low outgassing of volatiles, and can be easily modified for specific functions. Ag/cyanate ester based composites have received increased integration into electronic packaging processes because of its high reliability and processability. Die attachment materials made with cyanate-based matrix can be loaded with a multimodal mixture of Ag particles with filler loadings 90 wt% or more for increased thermal and electrical conductivity (2). However, cyanate-based die attach materials have a very high modulus not suitable for die attach. Modification of the polymer structure via copolymerization with a thermoplastic elastomer yields ECA with ideal toughness and flexibility for use as a die attach material. Modified cyanate-based ECAs have the ideal properties (low modulus, good thermal stability, low moisture outgassing, and limited popcorning) for use as a die attach material. The future of die attachment will require increased adhesive

performance. Advanced packages will require smaller, thinner, and lower cost packages for high performance mobile consumer devices. As devices move away from low profile quad flat packages to ball and grid array and CSP die attach will have to occur much closer to bond pads. Generally, electrically conductive composite films with good adhesion properties are used to minimize bleeding of adhesive paste eliminating contamination of pads. However, as chips become thinner and larger many technical challenges for die attach materials will arise. These include increased chip warpage caused by thermal expansion mismatch between silicon chip and polymer substrate, lower temperature stability of polymer substrate, and increased moisture absorption caused by thin package. Future developments in conductive composites for die attach will attempt to address these issues.

Flip Chip Applications. A second common application for electrically conductive composites is in flip chip interconnection. In traditional flip chip interconnection, solder bumps are used to make electrical connection between chip bumps and carrier pads. To achieve sufficient reliability underfill is required to fill the gap between the chip and chip carrier. The underfill creates a monolithic structure that distributes stresses over all surfaces, rather than just the solder joints. The distribution of stress prevents mechanical failure and cracking. ECAs more specifically ICAs are ideal materials for low cost flip chip technologies. ICAs offer numerous advantages including

(i) simplification of processing;
(ii) reduced thermal loads on components and wires;
(iii) modifiable polymer matrix and metallic fillers; and
(iv) minimal requirements for under bump materials because alloy formation is not a concern.

Flip chip interconnects can be designed with or without metallic bumps. For unbumped flip chip interconnects, ICA is screen printed through a metallic mesh to form ICA bumps on pads. Similarly, a stencil-printing process can be used to form ICA bumps on pads. In the stencil-printing process, a metallic stencil is used to selectively print ICA bumps on pads. The difference between these two processes is that in stencil printing the metallic stencil is in intimate contact with the substrate. On the other hand, in screen-printing processes the metallic mesh floats slightly above the surface of the substrate. Stencil-printing and screen-printing processes are shown in Figure 19.

The pads for ICA printing are generally Al coated with a thin layer of Ni/Au to prevent formation of nonconductive aluminum oxide. Both screen printing and stencil printing of ICA bumps offer an attractive low cost alternative to metallized bumps. The bump printing process involves screen-printing ICA directly onto the pads through a patterned metallic stencil or mesh. These stencils/meshes are generally fabricated by etching, electroforming, or laser drilling. During the printing process, a squeegee is used to push ICA through a designed stencil or mesh. As the stencil/mesh lifts away from the substrate, the patterned ICA paste remains. The ICA bumps that are formed via the screen-printing process can be either fully cured bumps (Fig. 20**a**) or precured (B-stage) bumps (Fig. 20**b**) for thermosetting polymers or alternatively can undergo a bakeout to remove residual solvent in

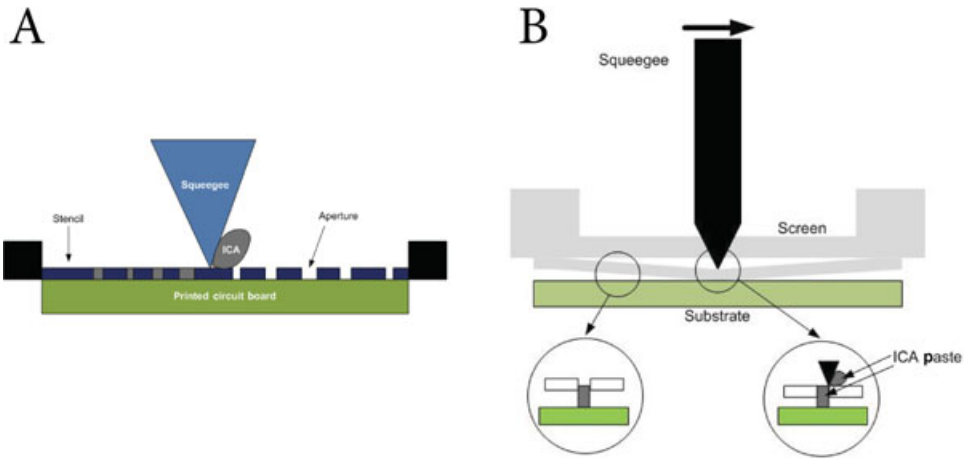

Fig. 19. (**A**) Stencil printing process; (**B**) screen-printing process.

thermoplastic ICAs (Fig. 20**c**). The bumps formed during this process are typically 50–75 μm. This process can create bumps with pitch as fine as 5 mils with bump densities up to 80,000 bumps/wafer. Once wafers are bumped and diced, wafers are flipped over and bonded to carrier chips. The bonding process is dependent on the material properties of the adjoining bumps. Following bonding, an underfill is injected into the gap between the chip and the carrier for mechanical reliability and environmental protection. ICA-based interconnection can also be made with metal-bumps. However, because these materials are isotropically conductive ICA must be selectively applied to only those areas where electrical interconnection is needed. Screen printing or stencil printing is commonly used to deposit ICA. To achieve fine a pitch interconnection, a very accurate stencil/substrate alignment is required. To overcome this issue a transfer method was developed by Matsushita (177) (Fig. 21). In this method, raised planarized Au studs are deposited on the die. These bumps are deposited by a ball-bumping process followed by a subsequent planarization. This process is highly efficient and eliminates the need for typical bumping processes, involving sputtering and plating processes. The ICA is then stencil printed into a thin film and transfer printed onto the stud surface. The transfer film thickness is controlled by the thin film thickness. The die is then aligned and cured on the carrier chip. Filling the cavity with underfill completes the assembly process. This method of flip chip interconnection has the unique capability of being oven curable because application of pressure is not required during assembly.

A final technique to create flip chip interconnections involves micromachining of bumps (178) (Fig. 22). In this process, a Cr/Au metallic pad is deposited on the silicon wafer. Patterning of the substrate is done using a thick photoresist. Following lithography, thermoplastic ICA is stencil printed into the preformed pattern. Because the difference in curing parameters of the ICA and the photoresist curing the photoresist can be stripped from the wafer, leaving behind dried ICA bumps. Bonding is completed by aligning the chip on the carrier wafer and curing at temperatures $\sim$20°C above the polymers melting temperature. Upon

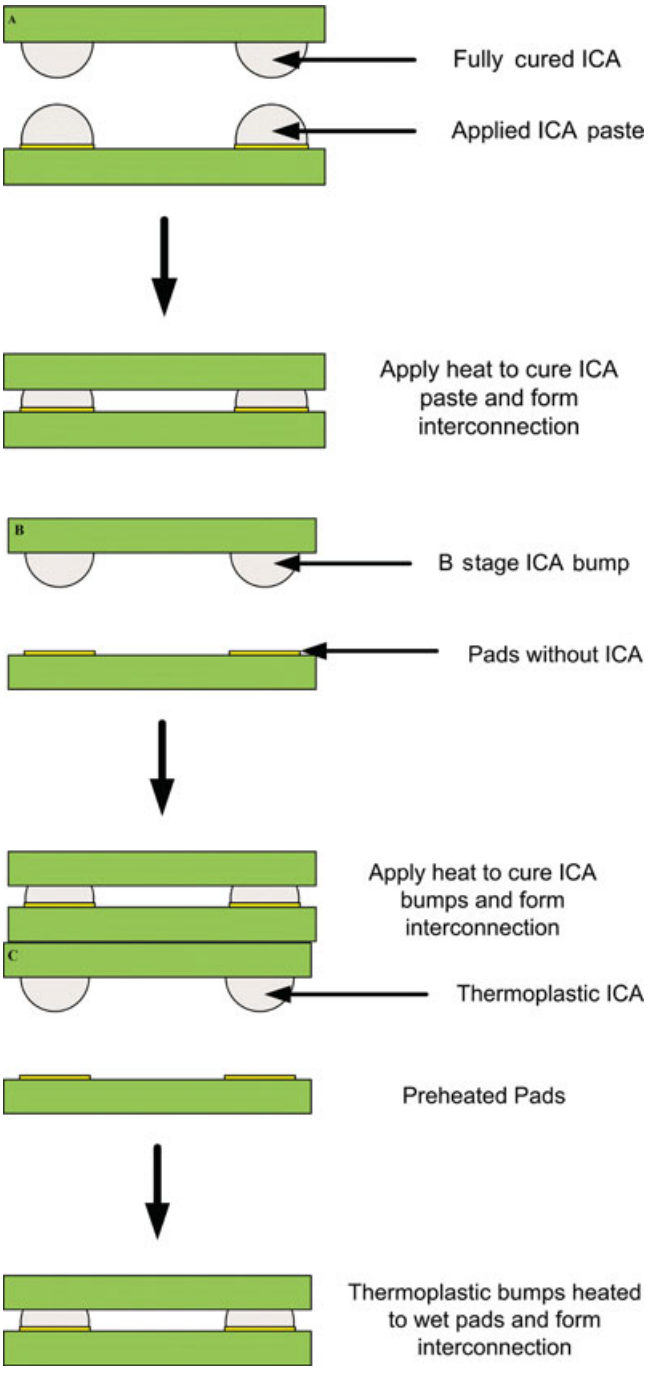

Fig. 20. Schematic drawings of die attachment assembly utilizing (**a**) chips with cured ICA bumps mated with uncured ICA, (**b**) B-stage ICA bumps, and (**c**) thermoplastic ICA bumps.

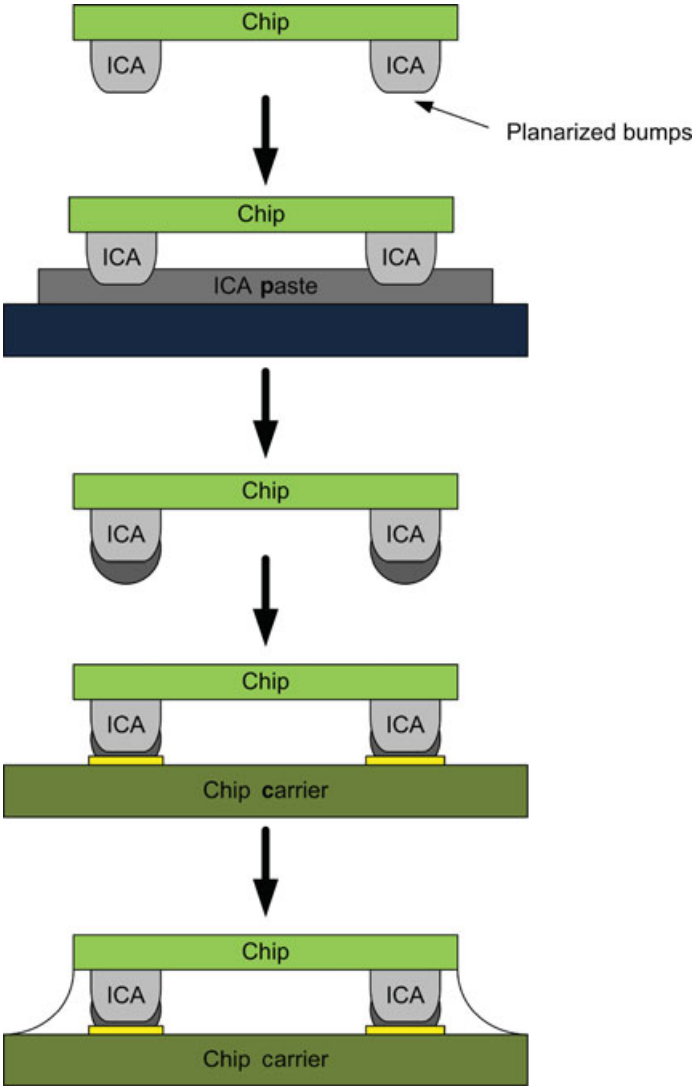

Fig. 21. Schematic drawing of flip chip attachment with planarized bumps.

cooling, mechanical and electrical interconnection is established. To enhance electrical and mechanical properties, pressure can be applied to the chip during bonding. Following filling the cavity with the underfill, the assembly is complete. As polymeric-based composite technologies continue to find ways to outperform inorganic materials, the electronic packaging industry will only become further dominated by electrically conductive polymer composites.

Summary

We have summarized recent advances of ICAs as a promising lead-free alternative to metal solders for electronic packaging applications. In the past few

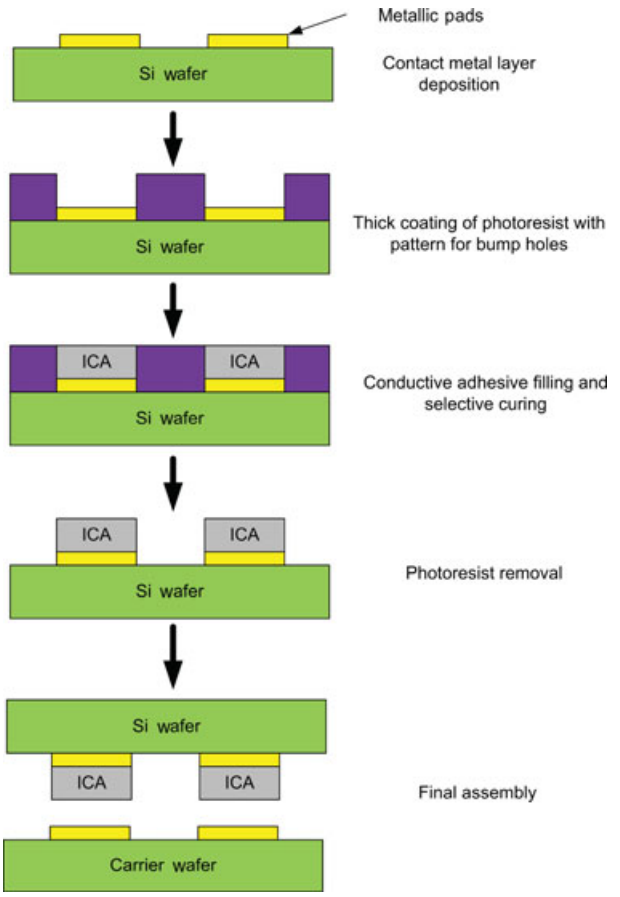

Fig. 22. Assembly via micromachined bumps.

years, remarkable progress has been made to meet the demands of the electronic packaging industry. This progress has made the development of ICAs with better electrical and mechanical properties, lower processing temperatures, stronger adhesion, and improved reliability for electronic packaging such as die attach and flip-chip interconnections. Compared with metal solders, the low processing temperature of ICAs has become an increasingly significant advantage for the emerging printed electronics. Low processing temperature of ICAs enables the use of low cost, nonsolderable, and thermally sensitive substrates (such as plastics and paper) in printed electronics. In particular, flexible and stretchable ICAs with a combination of electrical, mechanical, and adhesive functions are essential for the development of flexible and stretchable electronics. Development of highly reliable, highly conductive, and low cost ICAs will facilitate the increased applications of ICA technology in consumer and commercial devices. Continued advances in ICA material properties, processing, and reliability will enable ICAs to replace metal solders universally.

BIBLIOGRAPHY

"Conductive Polymer Composites" in *EPST* 3rd ed., Vol. 5, pp. 652–697, by Daoqiang Lu, Shijian Luo, and C. P. Wong, Georgia Institute of Technology.

CITED PUBLICATIONS

1. Y. Li, K.-S. Moon, and C. P. Wong, *Science* **308**, 1419–1420 (2005).
2. Y. Li and C. P. Wong, *Mater. Sci. Eng. R: Rep.* **51**, 1–35 (2006).
3. D. Lu, S. Luo, and C. P. Wong, in *Encyclopedia of Polymer Science & Technology*, 3rd Ed., John Wiley & Sons, Inc., New York, 2003, Vol. 5, pp. 652–697.
4. J. H. Lau, C. P. Wong, N. C. Lee, and S. W. Ricky, eds., *Electronics Manufacturing with Lead-free, Halogen-free & Conductive-adhesive Materials*, McGraw-Hill Companies, Inc., New York, 2003.
5. J. S. Hwang, ed., *Environmental-Friendly Electronics: Lead-Free Technology* Electrochemical Publications Ltd., Port Erin, UK, 2001.
6. J. Liu, ed., *Conductive Adhesives for Electronics Packaging*, Electrochemical Publications Ltd., Port Erin, British Isles, UK, 1999.
7. K.-I. Chen and K.-L. Lin, in *Proceedings of the 4th International on Symposium Electronic Material Packaging*, Kiaohsiung, Taiwan, Dec. 2002, pp. 49–54.
8. N. Kumbhat, A. Choudhury, M. Raine, G. Mehrotra, P. M. Raj, R. Zhang, K.-S. Moon, R. Chatterjee, V. Sundaram, G. Meyer-Berg, C. P. Wong, and R. R. Tummala, in *Proceedings of the 59th IEEE Electronic Component and Technology Conference*, San Diego, Calif., May 2009, pp. 1479–1485.
9. H. Jiang, K.-S. Moon, R. Zhang, and C. P. Wong, in *the 7th International IEEE Conference on Polymers and Adhesives in Microelectronics and Photonics (Polytronic 2008)*, Garmish-Partenkirchen, Germany, Aug. 2008, pp. 1–5.
10. Y. Li, K.-S. Moon, and C. P. Wong, *J. Appl. Polym. Sci.* **99**, 1665–1673 (2006).
11. K. Jain, M. Klosner, M. Zemel, and S. Raghunandan, *Proc. IEEE* **93**, 1500–1510 (2005).
12. J. Roncali, P. Leriche, and A. Cravino, *Adv. Mater.* **19**, 2045–2060 (2007).
13. R. Zhang, W. Wang, K. S. Moon, H. Jiang, W. Lin, and C. P. Wong, in *the 7th International IEEE Conference on Polymers and Adhesives in Microelectronics and Photonics (Polytronic 2008)*, Garmish-Partenkirchen, Germany, Aug. 2008, pp. 1–5.
14. J. C. Agar, K. J. Lin, R. Zhang, J. Durden, K.-S. Moon, and C. P. Wong, in *Proceedings of the 60th IEEE Electronic Component and Technology Conference*, Las Vegas, Nev., Jun. 2010, pp. 1226–1230.
15. Y. Li, M. J. Yim, K.-S. Moon, R. Zhang, and C. P. Wong, in *Proceedings of the 58th IEEE Electronic Component and Technology Conference*, Orlando, Fla., May 2008, pp. 1272–1276.
16. R. Zhang, Y. Duan, W. Lin, K. Moon, and C. P. Wong, in *Proceedings of the 59th IEEE Electronic Component and Technology Conference*, San Diego, Calif., May 2009, pp. 1356–1360.
17. K. Gilleo, in J. S. Hwang, ed., *Environmental-Friendly Electronics: Lead-Free Technology*, Electrochemical publications Ltd., Port Erin, UK, 2001, pp. 590–662.
18. D. D. Lu, Y. G. Li, and C. P. Wong, *J. Adhes. Sci. Technol.* **22**, 815–834 (2008).
19. M. J. Yim, Y. Li, K.-S. Moon, K. W. Paik, and C. P. Wong, *J. Adhes. Sci. Technol.* **22**, 1593–1630 (2008).
20. M. J. Yim and K. W. Paik, *Int. J. Adhes. Adhes.* **26**, 304–313 (2006).
21. I. Mir and D. Kumar, *Int. J. Adhes. Adhes.* **28**, 362–371 (2008).

22. L. J. Matienzo, R. N. Das, and F. D. Egitto, *J. Adhes. Sci. Technol.* **22**, 853–869 (2008).
23. D. D. Lu and C. P. Wong, *J. Adhes. Sci. Technol.* **22**, 835–851 (2008).
24. Y. C. Lin and X. Chen, *J. Adhes. Sci. Technol.* **22**, 1631–1657 (2008).
25. H. J. Lewis and A. Ryan, *J. Adhes. Sci. Technol.* **22**, 893–913 (2008).
26. R. Zhang, Y. Li, M. J. Yim, K. S. Moon, D. D. Lu, and C. P. Wong, *IEEE Trans. Compon. Packag. Technol.* **32**, 677–683 (2009).
27. J. E. Morris, Ed., *Nanopackaging: Nanotechnologies and Electronics Packaging*, Springer, Berlin, 2008.
28. D. Klosterman, L. Li, and J. E. Morris, *IEEE Trans. Compon. Packag. Manuf. Technol. A* **21**, 23–31 (1998).
29. J. Liu, *Soldering Surf. Mount Technol.* **13**, 39–57 (2001).
30. C. P. Wong, W. Lin, L. Zhu, H. Jiang, R. Zhang, Y. Li, and K. Moon, *Front. Optoelectron. China* **3**, 139–142 (2010).
31. C. T. Murray, R. L. Rudman, M. B. Sabade, and A. V. Pocius, *MRS Bull.* **28**, 449–454 (2003).
32. Y. C. Lin and J. Zhong, *J. Mater. Sci.* **43**, 3072–3093 (2008).
33. S. I. Asai, U. Saruta, M. Tobita, M. Takano, and Y. Miyashita, *J. Appl. Polym. Sci.* **56**, 769–777 (1995).
34. D. D. Chang, P. A. Crawford, J. A. Fulton, R. McBride, M. B. Schmidt, R. E. Sinitski, and C. P. Wong, *IEEE Trans. Compon. Hybrids, Manuf. Technol.* **16**, 828–835 (1993).
35. J. J. Licari and D. W. Swanson, *Adhesives Technology for Electronic Applications*, William Andrew, Norwich, N.Y., 2005.
36. M. J. Yim, Y. Li, K. S. Moon, and C. P. Wong, *J. Electron. Mater.* **36**, 1341–1347 (2007).
37. Y.-S. Lin and S.-S. Chiu, *Polym. Eng. Sci.* **44**, 2075–2082 (2004).
38. Y.-S. Lin and S.-S. Chiu, *J. Adhes. Sci. Technol.* **22**, 1673–1697 (2008).
39. R. Zhang, W. Lin, K. Lawrence, and C. P. Wong, *Int. J. Adhes. Adhes.* **30**, 403–407, (2010).
40. R. Zhang, W. Lin, K.-S. Moon, and C. P. Wong, *IEEE Trans. Adv. Packag.*, accepted.
41. J.-C. Huang, *Adv. Polym. Tech.* **21**, 299–313 (2002).
42. R. Zhang and F. Liu, *Polym. Mater. Sci. Eng.* **21**, 45–49 (2005).
43. S. Stankovich, D. A. Dikin, G. H. B. Dommett, K. M. Kohlhaas, E. J. Zimney, E. A. Stach, R. D. Piner, S. T. Nguyen, and R. S. Ruoff, *Nature* **442**, 282–286 (2006).
44. X. Wang, L. Zhi, and K. Muellen, *Nano Lett.* **8**, 323–327 (2008).
45. Y. Kim, S. Y. Cho, Y. S. Yun, and H.-J. Jin, *Mod. Phys. Lett. B* **23**, 3739–3745 (2009).
46. M. Heimann, M. Wirts-Ruetters, B. Boehme, and K.-J. Wolter, in *Proceedings of the 58th IEEE Electronic Component and Technology Conference*, Orlando, Fla., 2008, pp. 1731–1736.
47. X. Yu, R. Rajamani, K. A. Stelson, and T. Cui, *J. Nanosci. Nanotechnol.* **6**, 1939–1944 (2006).
48. M. Moniruzzaman and K. I. Winey, *Macromolecules* **39**, 5194–5205 (2006).
49. Y. Oh, D. Suh, Y. Kim, E. Lee, J. S. Mok, J. Choi, and S. Baik, *Nanotechnology* **19**, 495602 (2008).
50. H. P. Wu, X. J. Wu, M. Y. Ge, G. Q. Zhang, Y. W. Wang, and J. Jiang, *Compos. Sci. Technol.* **67**, 1182–1186 (2007).
51. J. Jang and S. K. Ryu, *J. Mater. Process. Technol.* **180**, 66–73 (2006).
52. M. You, L. Zhang, Z. Gong, W. Liu, and A. He, *Key Eng. Mater.* **373–374**, 220–223 (2008).
53. W. Lin, X. Xi, and C. Yu, *Synth. Met.* **159**, 619–624 (2009).
54. T. Liang, W. Guo, Y. Yan, and C. Tang, *Int. J. Adhes. Adhes.* **28**, 55–58 (2007).
55. G. Lu, X. Li, and H. Jiang, *Compos. Sci. Technol.* **56**, 193–200 (1996).
56. H. Zou, L. Zhang, M. Tian, S. Wu, and S. Zhao, *J. Appl. Polym. Sci.* **115**, 2710–2717 (2010).

57. S. K. Kang, R. S. Rai, and S. Purushothaman, *IEEE Trans. Compon. Packag. Manuf. Technol., A* **21**, 18–22 (1998).
58. D. Lu and C. P. Wong, *IEEE Trans. Electron. Packag. Manuf.* **23**, 185–190 (2000).
59. C. Gallagher, G. Matijasevic, and J. F. Maguire, in *Proceedings of the 47th Electronic Components and Technology Conference*, San Jose,Calif.. May 1997, pp. 554–560.
60. C. Shearer, B. Shearer, G. Matijasevic, and P. Gandhi, *J. Electron. Mater.* **28**, 1319–1326 (1999).
61. J.-M. Kim, K. Yasuda, and K. Fujimoto, *J. Electron. Mater.* **33**, 1331–1337 (2004).
62. S. K. Kang and S. Purushothaman, *J. Electron. Mater.* **28**, 1314–1318 (1999).
63. S. M. Pandiri, *Adhes. Age.* **30**, 31–35 (1987).
64. D. Lu and C. P. Wong, *J. Therm. Anal. Calorim.* **59**, 729–740 (2000).
65. D. Lu and C. P. Wong, *J. Therm. Anal. Calorim.* **61**, 3–12 (2000).
66. D. Lu, Q. K. Tong, and C. P. Wong, *IEEE Trans. Compon. Packag. Technol.* **22**, 365–371 (1999).
67. H. Dong, Y. Li, M. J. Yim, K. S. Moon, and C. P. Wong, *Appl. Phys. Lett.* **90**, 092102 (2007).
68. G. R. Ruschau, S. Yoshikawa, and R. E. Newnham, *J. Appl. Phys.* **72**, 953–959 (1992).
69. R. Holm, *Electric Contacts: Theory and Application*, Springer, New York, 1967.
70. H. P. Wu, X. J. Wu, M. Y. Ge, G. Q. Zhang, Y. W. Wang, and J. Z. Jiang, *Compos. Sci. Technol.* **67**, 1116–1120 (2007).
71. R. Zhang, K.-S. Moon, W. Lin, and C. P. Wong, in *Proceedings of the 59th IEEE Electronic Component and Technology Conference*, San Diego, Calif., May 2009, pp. 2034–2038.
72. I. A. Chmutin, S. V. Letyagin, V. G. Shevchenko, and A. T. Ponamorcnko, *Vysokomol. Soedin. Ser. A* **36**, 699–713 (1994).
73. V. I. Roldughin and V. V. Vysotskii, *Prog. Org. Coat.* **39**, 81–100 (2000).
74. V. E. Gul, *New Concepts in Polymer Science: Structure and Properties of Conducting Polymer Composites*, VSP, Utrecht, The Netherlands, 1996.
75. K. Gilleo, *Soldering Surf. Mount Technol.* **19**, 12–17 (1995).
76. P. G. Harris, *Soldering Surf. Mount Technol.* **20**, 19–21,26 (1995).
77. D. Lu, Q. K. Tong, and C. P. Wong, *IEEE Trans. Electron. Packag. Manuf.* **22**, 223–227 (1999).
78. D. Lu and C. P. Wong, *Int. J. Adhes. Adhes.* **20**, 189–193 (2000).
79. Y. Li, K.-S. Moon, and C. P. Wong, *IEEE Trans. Compon. Packag. Technol.* **29**, 173–178 (2006).
80. Y. Li, K.-S. Moon, A. Whitman, and C. P. Wong, *IEEE Trans. Compon. Packag. Technol.* **29**, 758–763 (2006).
81. H. P. Wu, J. F. Liu, X. J. Wu, M. Y. Ge, Y. W. Wang, G. Q. Zhang, and J. Z. Jiang, *Int. J. Adhes. Adhes.* **26**, 617–621 (2006).
82. Y. Tao, Y. Xia, H. Wang, F. Gong, H. Wu, and G. Tao, *IEEE Trans. Adv. Packag.* **32**, 589–592 (2009).
83. D. Chen, X. Qiao, X. Qiu, F. Tan, J. Chen, and R. Jiang, *J. Mater. Sci.: Mater. Electron.* **21**, 486–490.
84. X. Lin and F. Lin, in *Proceedings of the 6th IEEE Conference on High Density Microsystem Design and Packaging and Failure Analysis*, Shanghai, China, July 2004, pp. 382–384.
85. O. H. Kwon and G. L. Messing, *Acta Metall. Mater.* **39**, 2059–2068 (1991).
86. M. M. Hou and T. W. Eagar, *J. Electron. Packag.* **114**, 443–447 (1992).
87. R. N. Das, F. D. Egitto, and V. R. Markovich, *Circuit World*, **34**, 3–12 (2008).
88. K.-S. Moon, H. Dong, R. Maric, S. Pothukuchi, A. Hunt, Y. Li, and C. P. Wong, *J. Electron. Mater.* **34**, 168–175 (2005).

89. J. G. Bai, T. G. Lei, J. N. Calata, and G.-Q. Lu, *J. Mater. Res.* **22**, 3494–3500 (2007).
90. T. Wang, X. Chen, G.-Q. Lu, and G.-Y. Lei, *J. Electron. Mater.* **36**, 1333–1340 (2007).
91. H. Jiang, K.-S. Moon, Y. Li, and C. P. Wong, *Chem. Mater.* **18**, 2969–2973 (2006).
92. E. Ide, S. Angata, A. Hirose, and K. F. Kobayashi, *Acta Mater.* **53**, 2385–2393 (2005).
93. I. Reinhold, C. E. Hendriks, R. Eckardt, J. M. Kranenburg, J. Perelaer, R. R. Baumann, and U. S. Schubert, *J. Mater. Chem.* **19**, 3384–3388 (2009).
94. J. Perelaer, A. W. M. de Laat, C. E. Hendriks, and U. S. Schubert, *J. Mater. Chem.* **18**, 3209–3215 (2008).
95. T. H. J. van Osch, J. Perelaer, A. W. M. de Laat, and U. S. Schubert, *Adv. Mater.* **20**, 343–345 (2008).
96. A. Kamyshny, M. Ben-Moshe, S. Aviezer, and S. Magdassi, *Macromol. Rapid Commun.* **26**, 281–288 (2005).
97. P. Calvert, *Chem. Mater.* **13**, 3299–3305 (2001).
98. J. R. Greer and R. A. Street, *Acta Mater.* **55**, 6345–6349 (2007).
99. A. L. Dearden, P. J. Smith, D.-Y. Shin, N. Reis, B. Derby, and P. O'Brien, *Macromol. Rapid Commun.* **26**, 315–318 (2005).
100. S. Magdassi, M. Grouchko, O. Berezin, and A. Kamyshny, *ACS Nano* **4**, 1943–1948 (2010).
101. D. Wakuda, M. Hatamura, and K. Suganuma, *Chem. Phys. Lett.* **441**, 305–308 (2007).
102. H.-H. Lee, K.-S. Chou, and Z.-W. Shih, *Int. J. Adhes. Adhes.* **25**, 437–441 (2005).
103. L. Ye, Z. Lai, J. Liu, and A. Tholen, *IEEE Trans. Electron. Packag. Manuf.* **22**, 299–302 (1999).
104. H. Jiang, K.-S. Moon, J. Lu, and C. P. Wong, *J. Electron. Mater.* **34**, 1432–1439 (2005).
105. R. Zhang, K.-S. Moon, W. Lin, and C. P. Wong, *J. Mater. Chem.* **20**, 2018–2023 (2010).
106. R. Zhang and C. P. Wong, in *Proceedings of the 59th IEEE Electronic Component and Technology Conference*, San Diego, Calif., May 2009, 150–154.
107. S. Iwama and T. Sahashi, *Jpn. J. Appl. Phys.* **19**, 1039–1044 (1980).
108. P.-Y. Silvert, R. Herrera-Urbina, N. Duvauchelle, V. Vijayakrishnan, and K. T. Elhsissen, *J. Mater. Chem.* **6**, 573–577 (1996).
109. L. Kvitek, A. Panacek, J. Soukupova, M. Kolar, R. Vecerova, R. Prucek, M. Holecova, and R. Zboril, *J. Phys. Chem. C* **112**, 5825–5834 (2008).
110. Y. Xiong, A. R. Siekkinen, J. Wang, Y. Yin, M. J. Kim, and Y. Xia, *J. Mater. Chem.* **17**, 2600–2602 (2007).
111. M. Chen, L.-Y. Wang, J.-T. Han, J.-Y. Zhang, Z.-Y. Li, and D.-J. Qian, *J. Phys. Chem. B* **110**, 11224–11231 (2006).
112. M. Yamamoto, Y. Kashiwagi, and M. Nakamoto, *Langmuir* **22**, 8581–8586 (2006).
113. M. Yamamoto and M. Nakamoto, *J. Mater. Chem.* **13**, 2064–2065 (2003).
114. S. Kotthaus, B. H. Guenther, R. Haug, and H. Schaefer, *IEEE Trans. Compon. Packag. Manuf. Technol. A* **20**, 15–20 (1997).
115. T.-Y. Dong, W.-T. Chen, C.-W. Wang, C.-P. Chen, C.-N. Chen, M.-C. Lin, J.-M. Song, I.-G. Chen, and T.-H. Kao, *Phys. Chem. Chem. Phys.* **11**, 6269–6275 (2009).
116. B. T. Nguyen, J. E. Gautrot, M. T. Nguyen, and X. X. Zhu, *J. Mater. Chem.* **17**, 1725–1730 (2007).
117. R. Zhang, W. Lin, K.-S. Moon, and C. P. Wong, *ACS Appl. Mater. Interfaces* **2**, 2637–2645 (2010).
118. A. N. Gent and G. R. Hamed, in *Encyclopedia of Polymer Science & Technology*, 2nd ed. John Wiley & Sons, New York, 1985, pp. 476–518.
119. R. J. Good, *J. Adhes.* **4**, 133–154 (1972).
120. S. Liong, C. P. Wong, and W. F. Burgoyne, Jr., *IEEE Trans. Compon. Packag. Technol.* **28**, 327–336 (2005).
121. K.-S. Moon, C. Rockett, C. Kretz, W. F. Burgoyne, and C. P. Wong, *J. Adhes. Sci. Technol.* **17**, 1785–1799 (2003).

122. K.-S. Moon, C. Rockett, and C. P. Wong, *J. Adhes. Sci. Technol.* **18**, 153–167 (2004).
123. J. C. Love, L. A. Estroff, J. K. Kriebel, R. G. Nuzzo, and G. M. Whitesides, *Chem. Rev.* **105**, 1103–1169 (2005).
124. H. J. Zwolinski M, Rubon H, Zaks Y., in *Proceedings of the 2 nd International Conference on Adhesive Joining and Coating Technology in Electronics Manufacturing*, Stockholm, Sweden, Jun. 1996, pp. 333–340.
125. D. Lu, Q. K. Tong, and C. P. Wong, *IEEE Trans. Electron. Packag. Manuf.* **22**, 228–232 (1999).
126. H. Li, K.-S. Moon, and C. P. Wong, *J. Electron. Mater.* **33**, 106–113 (2004).
127. M. K. Antoon, J. L. Koenig, and T. Serafini, *J. Polym. Sci., Polym. Phys. Ed.* **19**, 1567–1575 (1981).
128. M. K. Antoon and J. L. Koenig, *J. Polym. Sci., Polym. Phys. Ed.* **19**, 197–212 (1981).
129. D. Lu and C. P. Wong, *J. Appl. Polym. Sci.* **74**, 399–406 (1999).
130. H. Leidheiser Jr., *J. Coat. Technol.* **53**, 29–39 (1981).
131. P. A. Reardon, in *Corrosion'86*, paper no. 175, Natural Association of Corrosion Engineers, Houston, Tex., 1986.
132. P. A. Reardon and W. E. Bernahl, in *Corrosion'87, paper no. 438*, Natural Association of Corrosion Engineers, Houston, Tex., 1987.
133. M. G. Noack, in *Corrosion'89, paper no. 436*, Natural Association of Corrosion Engineers, Houston, Tex., 1989.
134. S. Romaine, in *Proceedings of the American Power Conference*, Chicago, Ill., Apr. 1986, pp. 1066–1073.
135. R. Subramanian and V. Lakshminarayanan, *Corros. Sci.* **44**, 535–554 (2002).
136. K.-S. Moon, S. Liong, H. Li, and C. P. Wong, *J. Electron. Mater.* **33**, 1381–1388 (2004).
137. U.S. Pat. 5180523 (1989), D. Durand, D. Vieau, A. L. Chu, and T. S. Weiu (to Poly-Flex Circuits, Inc.).
138. D. W. Marshall, *J. Adhes.* **74**, 301–315 (2000).
139. L. T. Shi, R. Saraf, and W. S. Huang, *Process. Adv. Mater.* **3**, 57–62 (1993).
140. S. K. Kang, S. L. Buchwalter, N. C. LaBianca, J. Gelorme, S. Purushothaman, K. Papathomas, and M. Poliks, *IEEE Trans. Compon. and Packag. Technol.* **24**, 431–435 (2001).
141. L.-N. Ho, H. Nishikawa, N. Natsume, T. Takemoto, K. Miyake, M. Fujita, and K. Ota, *J. Electron. Mater.* **39**, 115–123 (2010).
142. H. Nishikawa, S. Mikami, N. Terada, K. Miyake, A. Aoki, and T. Takemoto, in *Proceedings of the 2nd Electronics System Integration Technology Conference*, Greenwich, UK, 2008, pp. 825–828.
143. S.-Y. Park, T.-W. Yoon, C.-H. Lee, I.-B. Jeong, and S.-H. Hyun, *Mater. Sci. Forum* **534–536**, 933–936 (2007).
144. Y. S. Gong, C. Lee, and C. K. Yang, *J. Appl. Phys.* **77**, 5422–5425 (1995).
145. Y. Z. Hu, R. Sharangpani, and S.-P. Tay, *J. Vac. Sci. Technol. A* **18**, 2527–2532 (2000).
146. M. M. Antonijevic and M. B. Petrovic, *Int. J. Electrochem. Sci.* **3**, 1–28 (2008).
147. V. Brusic, M. A. Frisch, B. N. Eldridge, F. P. Novak, F. B. Kaufman, B. M. Rush, and G. S. Frankel, *J. Electrochem. Soc.* **138**, 2253–2259 (1991).
148. A. M. Fenelon and C. B. Breslin, *J. Appl. Electrochem.* **31**, 509–516 (2001).
149. E. Stupnisek-Lisac, A. Brnada, and A. D. Mance, *Corros. Sci.* **42**, 243–257 (2000).
150. M. N. Desai and S. S. Rana, *Anti-Corros. Methods Mater.* **20**, 16–20 (1973).
151. S. Abd El Wanees, *Anti-Corros. Methods Mater.* **41**, 3–7 (1994).
152. E. M. Sherif and S.-M. Park, *J. Electrochem. Soc. B* **152**, 428–433 (2005).
153. E. M. Sherif and S.-M. Park, *Electrochim. Acta* **51**, 4665–4673 (2006).
154. S. B. Chakraborty, T. K. Bandyopadhyay, and S. R. Chaudhuri, *Bull. Electrochem.* **8**, 111–113 (1992).

155. S. Patil, S. R. Sainkar, and P. P. Patil, *Appl. Surf. Sci.* **225**, 204–216 (2004).
156. V. Brusiz, M. Angelopoulos, and T. Graham, *J. Electrochem. Soc.* **144**, 436–442 (1997).
157. R. Vera, R. Schrebler, P. Cury, R. Rio, and H. Romero, *J. Appl. Electrochem.* **37**, 519–525 (2007).
158. M. I. Redondo and C. B. Breslin, *Corros. Sci.* **49**, 1765–1776 (2007).
159. P. Herrasti, A. I. del Rio, and J. Recio, *Electrochim. Acta* **52**, 6496–6501 (2007).
160. M. I. Redondo, E. Sanchez de la Blanca, M. V. Garcia, and M. J. Gonzalez-Tejera, *Prog. Org. Coat.* **65**, 386–391 (2009).
161. S. Chaudhari and P. P. Patil, *Electrochim. Acta* **53**, 927–933 (2007).
162. P. A. Kilmartin, L. Trier, and G. A. Wright, *Synth. Met.* **131**, 99–109 (2002).
163. P. Herrasti, F. J. Recio, P. Ocon, and E. Fatas, *Prog. Org. Coat.* **54**, 285–291 (2005).
164. M. Tiitu, A. Talo, O. Forsen, and O. Ikkala, *Polymer* **46**, 6855–6861 (2005).
165. A. Wokaun, A. Baiker, S. K. Miller, and W. Fluhr, *J. Phys. Chem.* **89**, 1910–1914 (1985).
166. E. Stupnisek-Lisac, D. Kopjar, and A. D. Mance, *Bull. Electrochem.* **14**, 10–15 (1998).
167. M. Inoue and K. Suganuma, *J. Electron. Mater.* **36**, 669–675 (2007).
168. M. Inoue, H. Muta, T. Maekawa, S. Yamanaka, and K. Suganuma, *J. Electron. Mater.* **37**, 462–468 (2008).
169. C. Li, E. T. Thostenson, and T.-W. Chou, *Compos. Sci. Technol.* **68**, 1227–1249 (2008).
170. Z. Zhang, M. Rouabhia, Z. Wang, C. Roberge, G. Shi, P. Roche, J. Li, and L. H. Dao, *Artif. Organs* **31**, 13–22 (2007).
171. S. Watcharotone, D. A. Dikin, S. Stankovich, R. Piner, I. Jung, G. H. B. Dommett, G. Evmenenko, S.-E. Wu, S.-F. Chen, C.-P. Liu, S. T. Nguyen, and R. S. Ruoff, *Nano Lett.* **7**, 1888–1892 (2007).
172. B. Fugetsu, E. Sano, M. Sunada, Y. Sambongi, T. Shibuya, X. Wang, and T. Hiraki, *Carbon* **46**, 1256–1258 (2008).
173. D. J. Lee and J. H. Oh, *Thin Solid Films*, **518**, 6352–6356, (2010).
174. M. Yamazaki, in *Proceedings of LSI Assembly Technology Forum, ISS Industrial Systems*, 1996.
175. J. M. Pujol, C. Prud'homme, M. E. Quenneson, and R. Cassat, *J. Adhes.* **27**, 213–229 (1989).
176. T. Yoshida, *Gekkan Semicond. World*, **5**, 72 (1994).
177. Y. Bessho, in *Proceedings of International Microelectronics Conference*, May 1990, pp. 183–189.
178. K. W. Oh and C. H. Ahn, *IEEE Trans. Adv. Packag.* **22**, 586–591 (1999).

RONGWEI ZHANG
C. P. WONG
School of Chemistry and Biochemistry
Georgia Institute of Technology
School of Materials Science and Engineering
Georgia Institute of Technology
Atlanta, Georgia

JOSH C. AGAR
School of Materials Science and Engineering
Georgia Institute of Technology
Atlanta, Georgia